Unclassified
SECURITY CLASSIFICATION OF THIS PAGE

DTIC FILE COPY COPY NO. 2

AD-A218 378

DTIC ELECTE FEB 27 1990 S D

DOCUMENTATION PAGE

Form Approved OMB No. 0704-0188

Unclassified	1b. RESTRICTIVE MARKINGS: none
2a. SECURITY CLASSIFICATION AUTH[ORITY]	3. DISTRIBUTION/AVAILABILITY OF REPORT: distribution unlimited; approved for public release (2)
2b. DECLASSIFICATION/DOWNGRADING SCHEDULE	
4. PERFORMING ORGANIZATION REPORT NUMBER(S): NEAR TR 410	5. MONITORING ORGANIZATION REPORT NUMBER(S): AFOSR-TR-90-0269
6a. NAME OF PERFORMING ORGANIZATION: Nielsen Engineering & Research, Inc.	6b. OFFICE SYMBOL (If applicable):
6c. ADDRESS (City, State, and ZIP Code): 510 Clyde Avenue, Mountain View, CA 94043-2287	7a. NAME OF MONITORING ORGANIZATION: Air Force Office of Scientific Research
	7b. ADDRESS (City, State, and ZIP Code): Bolling AFB, DC 20332-6448
8a. NAME OF FUNDING/SPONSORING ORGANIZATION: Air Force Office of Sci. Res.	8b. OFFICE SYMBOL (If applicable): NA
8c. ADDRESS (City, State, and ZIP Code): Building 410, Bolling AFB, DC 203332-6448	9. PROCUREMENT INSTRUMENT IDENTIFICATION NUMBER: C - F49620-88-0006
	10. SOURCE OF FUNDING NUMBERS: PROGRAM ELEMENT NO. 65502F; PROJECT NO. 3005; TASK NO. A1; WORK UNIT ACCESSION NO.

11. TITLE (Include Security Classification)

A Study of Supermaneuver Aerodynamics (Unclassified)

12. PERSONAL AUTHOR(S)
David Nixon and Laura C. Rodman

13a. TYPE OF REPORT	13b. TIME COVERED	14. DATE OF REPORT (Year, Month, Day)	15. PAGE COUNT
Final Technical	FROM 12/1/88 TO 12/1/89	1990 January 31	73

16. SUPPLEMENTARY NOTATION

17. COSATI CODES			18. SUBJECT TERMS (Continue on reverse if necessary and identify by block number)
FIELD	GROUP	SUB-GROUP	supermaneuver, flow control, boundary conditions, artificial intelligence
01	01		
20	04		

19. ABSTRACT (Continue on reverse if necessary and identify by block number)

The objective of this work is to develop a novel technique for studying transient separated flows, such as those typical for maneuvering aircraft. The ultimate goal of this research is to develop flow control techniques using the boundary conditions in a Navier-Stokes calculation. Once numerical boundary conditions are established, then their physical counterparts may be found. A subdomain technique was developed which allows the study of the effects of various boundary conditions on a local portion of the flowfield. A search technique, using artificial intelligence methods, was developed and was used to find the combination of boundary conditions that achieved the desired flow control. In addition, a two-dimensional boundary conditions theory for the steady Euler and Navier-Stokes equations was derived. A wide range of boundary conditions for the subdomains were tried without significant success. However, a boundary condition, based on Duhamel's equation, was found to be very promising in leading to a reduction of computer time.

20. DISTRIBUTION/AVAILABILITY OF ABSTRACT	21. ABSTRACT SECURITY CLASSIFICATION
☒ UNCLASSIFIED/UNLIMITED ☐ SAME AS RPT. ☐ DTIC USERS	Unclassified

22a. NAME OF RESPONSIBLE INDIVIDUAL	22b. TELEPHONE (Include Area Code)	22c. OFFICE SYMBOL
Capt. Henry Helin	(202) 767-0471	AFOSR/NA

DD Form 1473, JUN 86 — Previous editions are obsolete. — SECURITY CLASSIFICATION OF THIS PAGE

A STUDY OF SUPERMANUEVER AERODYNAMICS

David Nixon
Laura C. Rodman
Nielsen Engineering & Research, Inc.
510 Clyde Avenue
Mountain View, CA 94043-2287

31 January 1990

Final Report for Period 1 December 1988 - 1 December 1989

Approved for Public release; distribution unlimited

Prepared for:
Air Force Office of Scientific Research
Building 410
Bolling AFB, DC 20332-6448

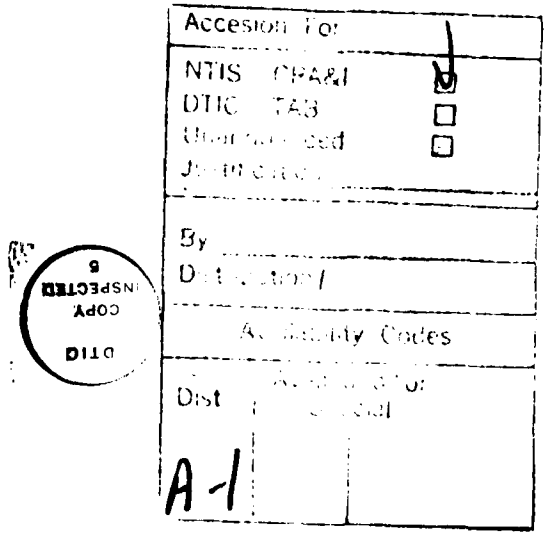

RESEARCH OBJECTIVES

The objective of this work is to develop a novel technique for studying transient separated flowfields, such as those typical for maneuvering aircraft. Transient aircraft maneuvers may result in augmented aerodynamic forces, yet difficulties in the prediction and control of these unsteady forces prevent them from being practically utilized. The ultimate goal of this research is to develop flow control techniques using the boundary conditions in a Navier-Stokes calculation as a guide.

In performing a Navier-Stokes calculation, the interior flow is determined by the boundary conditions specified at the edges of a domain (neglecting uncertainties such as the turbulence model, artificial dissipation effects, etc.). As only a few parameters can be specified on the boundaries, the variation of these conditions should allow the computation of any physical flowfield in the interior. A method of determining the boundary conditions which are capable of controlling unsteady separated flow is sought. Once numerical boundary conditions are established, then their physical counterparts may be found.

One objective is to compute the flow around a pitching, rolling wing to use as a secondary base on which to apply the flow control techniques described below. The primary base is a two-dimensional computation which is less expensive to use, but which contains a sufficient degree of flow complexity.

There are two further objectives in this work. The second objective is the development of a subdomain technique in a computational investigation. A subdomain of a flowfield is chosen such that it encompasses a flow phenomenon of interest. The boundary conditions of the subdomain allow a localized study of the effect of a certain flow parameter on the control of this portion of the flowfield. Also, the small grid associated with a subdomain (compared with a global solution which extends into the farfield) will lead to faster running times, which is necessary for time-intensive development work. An important aspect of research on the use of subdomains involves the determination of appropriate boundary conditions which will provide a consistent transition between a subdomain and a global calculation.

The third objective is the development of an intelligent search technique to find innovative boundary conditions. The purpose of this work is to find which boundary conditions will control a flowfield. As it is inefficient to randomly test new boundary conditions in the hope of discovering a useful one, a technique to methodically identify promising boundary conditions is required. A computerized search method, using artificial intelligence techniques, will search a field of possible boundary conditions in the most efficient manner. In addition, this computerized search technique may be standardized to be used in any flow situation.

STATUS OF RESEARCH EFFORT

Unsteady Flow Computations

The computation of the flow around a pitching, rolling wing was not achieved. This was due to two problems; first the construction of the correct boundary conditions for the subdomains proved much more difficult than expected, and second, there was considerable

uncertainty as to the availability of the computer resources to achieve this objective to adequate accuracy. The study was therefore restricted to the two-dimensional unsteady flow around an airfoil.

Subdomain Technique

The determination of appropriate boundary conditions for a subdomain calculation is an important aspect of this work. The flowfield at a subdomain boundary is generally two- or three-dimensional, and large gradients of velocity or thermodynamic quantities may exist. The widely-used[1] boundary condition theory for Navier-Stokes codes was developed for one-dimensional inviscid flow, and it is usually adequate for far-field boundary conditions when the flow is nearly one-dimensional. However, a multi-dimensional boundary condition theory is needed for a subdomain calculation. In addition, the boundary conditions for a subdomain must somehow be coupled with the flowfield within the subdomain. That is, if an upstream or airfoil surface boundary condition is altered in order to change the internal flowfield, the downstream boundary condition must also reflect the internal changes so as not to be physically inconsistent.

The boundary conditions most commonly used for Navier-Stokes computations are derived[1] from the one-dimensional inviscid gas dynamic equations. These boundary conditions are:

1. inflow: specify ρ, U, V and extrapolate p from the interior.
2. outflow: specify p and extrapolate ρ, U, and V from the interior.

Where U and V are the velocity components, ρ is the density and p is the pressure.

An analysis of boundary conditions for the two-dimensional steady Euler and Navier-Stokes equations has been completed.[2] This note is attached as Appendix A. The boundary conditions for the steady two-dimensional Euler equations are for an inflow boundary:

1. ρU or ρV is specified
2. ρ_∞ and p_∞ are specified (ρ_∞, p_∞ are datum values)
3. entropy is specified

At an outflow boundary, the entropy is extrapolated from the interior, rather than specified independently; otherwise the outflow boundary conditions are the same as those for inflow. For one-dimensional flow these boundary conditions reduce to the conditions given by Yee.[1] In Reference 2 the conditions are given for which one-dimensional boundary conditions are adequate. All quantities that are not specified are extrapolated from the interior solution.

The two-dimensional steady Navier-Stokes equations may be written in a form to show that the appropriate boundary conditions are:

1. ρU and ρV specified on a boundary
2. either entropy, pressure, or temperature specified on a boundary (allowing the computation of ρ), and
3. both ρ_∞ and p_∞ specified as a datum.

These conditions differ from those given in Reference 1 because the latter are derived from the one-dimensional inviscid Euler equations.

Having developed the boundary conditions it becomes a more than trivial matter to numerically implement them. In particular the correct boundary conditions for a subdomain are difficult to implement because it is almost impossible to specify values of ρU, ρV, and p on the subdomain boundary that are consistent with the flow in the adjoining subdomain. A wide range of existing boundary condition treatments were tested with little success; these techniques and extensions of these techniques are noted below.

Computations over a subdomain of a global solution field have shown that the interior flow solution for the subdomain is critically dependent on the outflow boundary conditions. For example, if the flow over the airfoil is separated, but the outflow boundary condition is attached flow, the interior flow will reattach before reaching the back boundary. This contrasts with the global solution, where the flow remains separated. A subdomain calculation such as the one just described will probably be unstable and will diverge after some time. All of the calculations that were performed with outflow boundary conditions that were physically inconsistent with the interior flow were unstable.

It is possible to reproduce a global solution in a subdomain if data from the global solution is used as the boundary conditions. However, using all of the global data that is available will overspecify the boundary conditions. If partial data is used for the boundary conditions instead, such as specifying three variables at an inflow and one at an outflow, the interior flow will be mostly reproduced, with the exception of the outflow regions. Those regions will be somewhat different from the global solution. If the boundary is in a region of high flow gradients, the more freedom that is allowed in specifying the boundary conditions, the more the boundary conditions will differ from the global data they were derived from. For instance, if the global data is used to provide boundary conditions in the form of the Riemann invariants, the resultant flow and boundary conditions will have enough flexibility to change significantly from the original global solution.

Boundary conditions applied in a wake region were investigated for use on a subdomain boundary. It was thought that formulating the boundary conditions in terms of the Riemann invariants would produce a reasonable result, since there is more flexibility in that formulation to allow the flow to adjust to the interior. One problem with this technique is that the Riemann invariants are derived for one-dimensional flow, and there is no corresponding formulation for two-dimensional flow. Consequently, there is some question as to what pseudo-one-dimensional velocity to choose in the formulation of the invariants. Either the normal velocity to the boundary or the total velocity seems to be the best choice, although there is no strict justification for either.

The formulation of these boundary conditions that is used in the NASA Ames Navier-Stokes code ARC2D is

$R1 = Q_n - 2a/(\gamma - 1)$	specified at inflow
$R2 = Q_n + 2a/(\gamma - 1)$	specified at outflow
entropy	specified at inflow
Q_t	specified at inflow

where Q_n and Q_t are the normal and tangential velocity components relative to the boundary.

This formulation was tried using either Q_n or Q_{total} in the equations for the Riemann invariants. It was found that in a wake, where there are large flow gradients present in the vicinity of the boundary, the changes in flow quantities between the first and second grid point were large enough to cause very large errors in the boundary conditions. For instance, for an inflow, R1 is specified at the boundary and R2 is extrapolated from one grid point away from the boundary. R1 and R2 are combined to solve for the speed of sound, a. Since the speed of sound is close to one, and the density goes as $(a^2)^{1/(\gamma-1)}$, a 2% error in the speed of sound leads to a 10% error in the density. Adding constraints, such as the removal of the dependence of the speed of sound on the Riemann invariants, improved the solution somewhat but still did not give satisfactory results.

From the analysis in Reference 2, certain flow quantities or their derivatives may be specified as boundary conditions. The boundary conditions can consist, therefore, of either setting a flow quantity, its first derivative, or its second derivative equal to zero on the boundary. These boundary conditions represent a case where all information is taken from the interior flow, regardless of whether there is inflow or outflow across the boundary. These boundary conditions were generally stable, but did not result in solutions which resembled the global solution.

An attempt was made to formulate the boundary conditions along a wake in terms of the vorticity and entropy, as these quantities are conserved along streamlines in two-dimensional inviscid flow. It was felt that using vorticity as a boundary condition would be convenient for flow control problems, since vortex generators are commonly used for flow control. The Riemann invariants were also needed to complete the boundary condition set. Unfortunately, since the vorticity must be integrated to find the velocities and the Riemann invariants only provide information on the total velocity, information about the sign of one of the velocity components is lost. Another problem with this formulation is that it appeared to be unstable for any slight perturbations in the solution, and it was thus unusable for a subdomain boundary condition.

Nonreflecting boundary conditions were investigated for use on the outflow boundary. These boundary conditions suppress reflections from outgoing waves and cancel incoming waves for a domain. Nonreflecting boundary conditions have been derived in the literature for hyperbolic equations on cartesian grids.[3] In this work, the boundary conditions were derived for use on curvilinear grids and were applied to low speed vortex shedding problems.[4,5] Appendices B and C describe the results from this work. Some of these results were also presented at the Minisymposium on Outflow Boundary Conditions, Swansea, United Kingdom, July 10, 1989.

The trials with nonreflecting boundary conditions showed that these conditions are inappropriate for subsonic vortex shedding flows. For a single vortex passing through a boundary, the convected quantities are computed satisfactorily, but the pressure is highly inaccurate. For a vortex street, the frequency of the vortex shedding is rapidly changed from the global solution.

The primary reason for the failure of the boundary conditions described above is that they fail to estimate adequately the flow outside the computational subdomain. Nonreflecting boundary conditions simply allow the perfect transmission of waves through the boundary but do not consider whether the boundary condition implies a physically unreasonable solution outside the computational domain. For certain conditions, a boundary condition that removes this uncertainty was derived during the present work. The idea is described briefly below; a more complete description is given in Appendix D.

If a particular flow is started from zero, then the flow in the exterior domain is exact until waves from the disturbance in the interior domain cross the boundary. If true nonreflecting boundary conditions could be devised, then the outflow boundary condition would be correct if the computation was started at zero time and is time accurate. An error in the boundary conditions due to approximations in the formulation can give rise to a nonphysical flow in the exterior domain and hence, ultimately, the interior domain. A principal difficulty is in finding an analytic relationship that will give the boundary conditions for the Navier-Stokes equations. The progress in nonreflecting boundary conditions shows that finding a true two-dimensional boundary condition is beyond the present state of the art.

The new idea is based on the following facts:

(a) If the solution is started from a zero disturbance state, then the outflow boundary condition is correct until the disturbance waves pass the boundary.

(b) The flow in the exterior domain is determined solely by its inflow boundary conditions which are compatible with the outflow boundary condition for the interior domain.

It is also assumed that the flow in the exterior domain can be constructed by a superposition of flow with linearized inflow boundary conditions. The range of validity of this assumption is not clear but the present results are very encouraging.

Based on these assumptions, the flow in the exterior domain is determined at each time step by the flow parameters on the penultimate grid line in the computational domain. The only part of the exterior flow that is important is that on the outflow boundary of the interior solution which is assumed to overlap with the exterior domain. The exterior flow is computed by relating the time dependent flow to a superposition of the flow due to a step change on the boundary (the indicial responses). Results for the unsteady transonic small disturbance equation for a pitching airfoil are given in Appendix D.

Flow Control and Optimization

Attempts were made to steady the vortex shedding process behind a stalled airfoil, in order to hold a vortex fixed over the upper surface. If a vortex could be held fixed or slowed down, the high lift over an airfoil could be controlled. Various combinations of jets or suction over the upper surface, both normal and tangential, were tried. It was also attempted to hold the vortex steady by fixing the instantaneous boundary conditions about a subdomain containing the vortex. None of these attempts worked. It does not seem to be possible to use steady flow-through boundary conditions for an unsteady flow, even if it is

desired to have the resultant solution be steady. Especially, it is not possible to use an instantaneous solution to an unsteady flow and for the boundary conditions to a steady flow. Since a solution to the unsteady Navier-Stokes equations is not necessarily a solution to the steady Navier-Stokes equations, then if a steady vortex flow can be found, it will probably be a somewhat different flowfield than what was started with. Flexible boundary conditions are necessary for consistency with the interior solution, and this leads to the problem of boundary condition specification again.

A study of optimization techniques was made to search for boundary conditions which have a controlling effect on a flowfield.[7] This study was made independently of the outflow boundary condition work. Since efficiency is a major concern when faced with the possibility of many iterations of a CFD solution, it was decided to use artificial intelligence search techniques rather than a purely mathematical optimizer.

A basic study with a mathematical optimizer was undertaken initially, in order to show that optimizing techniques may be used to find desirable sets of boundary conditions. The test problem was that of blowing over the upper rear surface of an airfoil. The magnitude of the blowing and the area were allowed to vary, and the objective was to maximize the lift coefficient and minimize the jet area. Although this was a simple test case, the results confirmed that mathematical optimizers are inefficient and tend to get stuck on local optima rather than on the global optimum.

The decision to use an artificial intelligence search technique was made because it could be programmed to give information about the various dependencies of the solution on the input variables, as well as the optimal values of the inputs. The technique that was developed here acts as a postprocessor on a series of CFD results. Each computation uses a slightly different input, and various results for each input are documented. The postprocessing technique then finds the dependencies of the results on each input and how the combination of inputs changes the solution.

This technique was tested on the flow control of an airfoil with unsteady separation. The airfoil has pulsed blowing or suction over the upper rear of the airfoil. The inputs that were varied with each calculation were the magnitude of the blowing or suction, the blowing pulse duration, and the interval between pulses. The objective was to increase the average forces on the airfoil and to decrease the rms forces. This technique found an optimum for a low suction magnitude and short duration and interval pulses. It also identified that the solution was most sensitive to the inputs for long blowing durations, short intervals between blowing pulses, and high suction values.

A detailed description of this method is found in Appendix E. This technique may be applied to any complex flow field and is not limited by the number of variables in the problem. The possibility exists of extending this technique to finding the interrelationships among several time-varying flow quantities, rather than between the output quantities and the input. This extension to the technique would find useful applications in areas such as turbulence modeling.

Summary

The main goal of the research reported here is to develop a method of flow control for highly maneuverable aircraft. The method used in the work is based on the idea that all flow control devices are represented by boundary conditions, and, therefore, only the small set of boundary conditions need be manipulated to achieve control rather than a large set of possible physical control devices. In order to determine the effect of a control on an element of the flow, for example, a vortex, the flow domain was divided into subdomains, each of which contained one or more flow features of interest. An artificial intelligence optimizer was developed to determine the best controls to use.

The work performed during the contract did achieve most of the tasks, such as the development of an intelligence optimizer and some insight into methods of control. The main stumbling block was the inadequate status of boundary conditions for the subdomains, a fact that was foreseen at the outset. None of the currently used boundary conditions in CFD proved to be satisfactory and only towards the end of the contract did a possible solution (the indicial boundary condition) appear. As an additional point, the use of this boundary condition could reduce computational time of CFD calculations considerably because of its capability of reducing the grid size substantially.

References

1. Yee, H. C.: Numerical Approximation of Boundary Conditions with Applications to Inviscid Equations of Gas Dynamics. NASA Technical Memorandum 81265, 1981.

2. Nixon, D.: Derivation of the Boundary Conditions for the Two-Dimensional Euler and Navier-Stokes Equations. Nielsen Engineering & Research Paper No. 262, 1989.

3. Thompson, K. W.: Time Dependent Boundary Conditions for Hyperbolic Systems. Journal of Computational Physics, Vol. 68, 1987, pp. 1-24.

4. Rodman, L. C.: The Application of Nonreflecting Boundary Conditions to 2-D Unsteady Computations on Curvilinear Grids. To be published as AIAA-90-1587, AIAA 21st Fluid Dynamics, Plasmadynamics, and Lasers Conference, Seattle, WA, June 18-20, 1990.

5. Rodman, L. C.: Outflow Boundary Conditions for Vortex Shedding Behind a Circular Cylinder. Nielsen Engineering & Research Paper No. 252, August 1989.

6. Nixon, D.: Outflow Boundary Conditions Using Duhamel's Equation. Abstract submitted to the AIAA 8th Applied Aerodynamics Conference, August 1990.

7. Rodman, L. C.: A Characterization and Search Technique for Unsteady Flow Control Problems. Abstract submitted to the AIAA 8th Applied Aerodynamics Conference, August 1990.

WRITTEN PUBLICATIONS

1. Nixon, D.: Outflow Boundary Conditions Using Duhamel's Equation. Abstract submitted to the AIAA 8th Applied Aerodynamics Conference, August 1990.

2. Nixon, D.: Derivation of the Boundary Conditions for the Two-Dimensional Euler and Navier-Stokes Equations. Nielsen Engineering & Research Paper No. 262, 1989.

3. Rodman, L. C.: The Application of Nonreflecting Boundary Conditions to 2-D Unsteady Computations on Curvilinear Grids. To be published as AIAA-90-1587, AIAA 21st Fluid Dynamics, Plasmadynamics, and Lasers Conference, Seattle, WA, June 18-20, 1990.

4. Rodman, L. C.: Outflow Boundary Conditions for Vortex Shedding Behind a Circular Cylinder. Nielsen Engineering & Research Paper No. 252, August 1989.

5. Rodman, L. C.: A Characterization and Search Technique for Unsteady Flow Control Problems. Abstract submitted to the AIAA 8th Applied Aerodynamics Conference, August 1990.

PROFESSIONAL PERSONNEL

Dr. David Nixon
Dr. Laura C. Rodman
Dr. Mohammad Farshchi
Dr. Gary D. Kuhn

INTERACTIONS

Discussions with Professor John Hughes (The Queens University at Belfast) and Dr. Alison Vogel (NASA Ames Research Center) have taken place. These discussions have involved the feasibility of applying A.I. techniques to this work.

DISCOVERIES

No new discoveries or patents have resulted from this work.

APPENDIX A

Derivation of the Boundary Conditions for the Two-Dimensional Euler and Navier-Stokes Equations

BOUNDARY CONDITIONS FOR THE EULER EQUATIONS

Introduction

This paper is concerned with deriving the necessary and sufficient boundary conditions for both the Euler and Navier-Stokes equations. In Part I, the boundary conditions for the Euler equations are developed for two-dimensional flow and are compared with the restrictions implied by the usual[1] outflow boundary conditions that are based on one-dimensional theory. It is shown that the commonly used characteristic boundary conditions are not generally relevant to multi-dimensional problems.

In Part II of this paper, the boundary conditions for the compressible, two-dimensional Navier-Stokes equations are derived.

Basic Equations

The vorticity equation

$$U_y - V_x = \omega$$

can be written in terms of a stream function ψ such that

$$\psi_{xx} + \psi_{yy} = \rho\omega + \rho_y U - \rho_x V \tag{1}$$

where ω is the vorticity and

$$\psi_y = \rho U - \rho_\infty U_\infty ; \psi_x = -\rho V \tag{2}$$

By manipulation of the energy and gas equations, and using Gibbs relation, the density is given in terms of the entropy, S, and the velocity components U, V by

$$\rho = \rho_\infty \left\{1 + \frac{(\gamma-1)}{2} M_\infty^2 \left[1 - \frac{U^2}{U_\infty^2} - \frac{V^2}{U_\infty^2}\right]\right\}^{\frac{1}{\gamma-1}} \exp(-S/R) \tag{3}$$

The vorticity is given by Crocco's theorem as

$$-\omega = \frac{T}{q}\frac{\partial S}{\partial n} = \frac{P}{R\rho q} \cdot \frac{\partial S}{\partial n} \tag{4}$$

where R is the gas constant

$$q = (U^2 + V^2)^{1/2}$$

and

$$\frac{\partial}{\partial n}$$

is the derivative in the direction normal to the streamlines. Note that

$$\frac{\partial}{\partial n} = \frac{U}{q}\frac{\partial}{\partial u} - \frac{V}{q}\frac{\partial}{\partial x} \tag{5}$$

Along a streamline the entropy is constant and hence

$$U\frac{\partial S}{\partial x} + V\frac{\partial S}{\partial y} = 0 \tag{6}$$

The pressure is given by

$$p = p_\infty \left\{1 + \frac{(\gamma-1)}{2} M_\infty^2 \left[1 - \frac{U^2}{U_\infty^2} - \frac{V^2}{U_\infty^2}\right]\right\}^{\frac{\gamma}{\gamma-1}} \exp(-S/R) \tag{7}$$

Using Equations (3), (4), (5), and (6), Equation (1) can be written as

$$\begin{aligned}\psi_{xx} + \psi_{yy} = &- \frac{p_\infty Q^{\gamma/\gamma-1}\exp(-S/R)}{Rq^2}\left(U\frac{\partial S}{\partial y} - V\frac{\partial S}{\partial x}\right) \\ &+ \rho_\infty \frac{\partial}{\partial y}\left[Q^{\frac{1}{\gamma-1}}\exp(-S/R)\right] U - \rho_\infty \frac{\partial}{\partial x}\left[Q^{\frac{1}{\gamma-1}}\exp(-S/R)\right]V\end{aligned} \tag{8}$$

where Q is a function of U and V and is given by

$$Q = \left[1 + \frac{(\gamma-1)}{2} M_\infty^2 \left(1 - \frac{U^2}{U_\infty^2} - \frac{V^2}{U_\infty^2}\right)\right] \tag{9}$$

Equation (8) can be written as

$$\psi_{xx} + \psi_{yy} = f(x, y) \tag{10}$$

where f(x, y) is the right hand side of Equation (8).

Consider the inviscid transonic problem illustrated in Figure 1. The solution is described by the Euler equations. We assume that the airfoil can be represented by specifying boundary conditions on the chord line, that is, thin airfoil boundary conditions are applied. An interesting example of a subdomain is as follows. The subdomain is defined as the region bounded by the lines AB, BC, CD, and DA.

Equation (10) can be written as an integral equation using Green's Theorem. Thus, in the domain D

$$\psi = + \int_{\xi_C}^{\xi_D} (K\psi_\eta - K_\eta\psi)\,d\xi + \int_{\eta_B}^{\eta_C} (K\psi_\xi - K_\xi\psi)\,d\eta$$

$$+ \int_{\xi_A}^{\xi_B} (K\psi_\eta - K_\eta\psi)\,d\xi - \int_{\eta_D}^{\eta_A} (K\psi_\xi - K_\xi\psi)\,d\eta + \int_D\int Kf\,dS \qquad (11)$$

where the kernel function K is given by

$$K = \frac{1}{2\pi} \ln[(x - \xi)^2 + (y - \eta)^2]^{1/2} \qquad (12)$$

Differentiation of Equation (11) with respect to y gives

$$\psi_y = \rho U - \rho_\infty U_\infty = - \int_{\xi_C}^{\xi_D} \{\tilde{\Delta}(K_y\psi_\eta) - \tilde{\Delta}(K_x\psi_\xi)\}\,d\xi$$

$$+ \int_{\eta_B}^{\eta_C} (K_y\psi_\xi + K_x\psi_\eta)\,d\eta + \int_D\int K_y f\,dS$$

$$- \int_{\eta_D}^{\eta_A} (K_y\psi_\xi + K_x\psi_\eta)\,d\eta \qquad (13)$$

$$+ K_x\psi\Big|_A^B - K_x\psi\Big|_B^C - K_x\psi\Big|_C^D + K_x\psi\Big|_D^A$$

where

$$\tilde{\Delta}f = f_{AB} - f_{CD} \qquad (14)$$

If the mass fluxes are known on the boundaries then the line integrals are known. These are the necessary boundary conditions for the subproblem.

Differentiation of Equation (11) with respect to x gives

$$\psi_x = -\rho V = -\int_{\xi_C}^{\xi_D} \{\tilde{\Delta}\ (K_x\psi_\eta) + \tilde{\Delta}\ (K_y\psi_\xi)\}\ d\xi + \int_{\eta_B}^{\eta_C} \{K_x\psi_\xi + K_y\psi_\eta\}\ d\eta$$

$$- \int_{\eta_D}^{\eta_A} \{K_x\psi_\xi + K_y\psi_\eta\}\ d\eta + \int_D\int K_x f ds \qquad (15)$$

$$+ \left.K_y\psi\right|_A^B - \left.K_y\psi\right|_B^C - \left.K_y\psi\right|_C^D + \left.K_y\psi\right|_D^A$$

From Equations (3) and (8) it can be seen that ρ and f are functions only of U and V and the entropy S. The entropy is given by Equation (6) and the velocities just ahead of the shock wave. Thus S is a function only of U and V. Hence, if ρV is defined on $y = \pm 0$ as a boundary condition, Equation (13) and (15) are equations for U and V throughout the flow field. Because of the complexity of the relations for ρ, S, and f, it is not easy to determine the number of possible solutions. However, it is safe to say that if ρV or ρU is specified on the boundary, then ρU and ρV are determined completely in the flow field. ρU is also determined on the boundary. In other words, U and V cannot both be specified on the boundary.

If a constant pressure boundary condition is used then Crocco's equation gives

$$\frac{\rho\ \omega}{\rho_\infty U_\infty} = -\frac{\rho^\gamma/\rho_\infty^\gamma}{\gamma\ R\ M_\infty^2}\ \exp\ (\Delta S/C_v)\ \frac{\partial \Delta S}{\partial \eta} \qquad (16)$$

where R is the gas constant, C_v the specific heat at constant volume, and ΔS is the entropy due to the shock wave. If a small disturbance approximation is made such that only linear terms involving v are retained, then a study of the density-velocity relation gives

$$\frac{\rho_\eta U}{\rho_\infty U_\infty} = \frac{p}{p_\infty}\ (\gamma-1)\ M_\infty^2\ \frac{U_\eta U^2}{U_\infty^3}\ \{1 + \frac{(\gamma-1)}{2}\ M_\infty^2\ (1 - \frac{U^2}{U_\infty^2})\}^{-2}$$

$$+ \frac{U}{U_\infty}\ (p/p_\infty)_\eta\ \{1 + (\frac{\gamma-1}{2})\ M_\infty^2\ (1 - \frac{U^2}{U_\infty^2})\}^{-1} \qquad (17)$$

and hence on the boundary, if p is constant

$$f(q,\eta) = \rho\omega + \rho_\eta U = (\rho U)_\eta \qquad (18)$$

On the boundary, Equation (13) therefore reduces to an equation for ρU in terms of ρV.

It is of interest to assume one-dimensional flow for comparison. In this case, conditions are uniform across DA and the vorticity is zero. Therefore, f is zero and Equation (13) can have the solution

$$\rho U|_{\xi_D} = \rho(p,\Delta S)U(p,\Delta S)|_{\xi_D} = \text{constant}. \qquad (19)$$

From Equation (7), the one-dimensional equation gives

$$\frac{U}{U_\infty} = \{1 - \frac{2}{(\gamma-1)M_\infty^2} \cdot [\ (p/p_\infty)^{\frac{\gamma-1}{\gamma}} \cdot \exp(S/R)^{\frac{\gamma-1}{\gamma}} - 1\ ]\ \}^{1/2} \qquad (20)$$

and hence, using Equation (3)

$$\frac{\rho U}{\rho_\infty U_\infty} = \frac{p}{p_\infty} \exp(-S/R)^{\frac{\gamma-1}{\gamma}} \{1 - (\frac{2}{(\gamma-1)M_\infty^2})([\ (\frac{p}{p_\infty}) \exp(S/R)\ ]^{\frac{\gamma-1}{\gamma}} - 1\ )\}^{1/2} \qquad (21)$$

and Equation (19) becomes an equation for the entropy S in terms of the given p. If S is known, U is found from Equation (20) and ρ is found from Equation (3). Thus all of the unknowns at the outflow boundary are found in terms of the specified pressure.

Inflow Boundary Conditions

For the above analysis of boundary conditions to be applicable the properties of the fluid must be specified. The most obvious place to specify this is at the inflow boundary. Thus at the inflow boundary the following must be specified

(a)	ρU or ρV	($\rho_\infty U_\infty$ in the above context)
(b)	ρ	(ρ_∞ in the above context)
(c)	p	(p_∞ in the above context)

Outflow Boundary Conditions

At the downstream boundary ρV (say) is specified, and if p is a constant, then Equation (13) is an equation for ρU on the boundary. The entropy is given by the internal solution which then gives ρ. Thus at the outflow boundary the following must be specified.

(a)	p
(b)	ρV (or ρU)

The other quantities are found from the solution (i.e., extrapolation)

Use of One-Dimensional Boundary Conditions

Equation (13) reduces to the one-dimensional equation if f and V are zero. Hence one-dimensional boundary conditions may be applicable if

$$|\rho V| << 1 \tag{22}$$

and if

$$|f| = |\rho\omega + \rho_\eta U| << 1 \tag{23}$$

Thus the "crossflow" on the boundary must be small and the vorticity must be small. Extropolation in the x direction cannot be used if $\frac{\partial f}{\partial x}$ is not small, and from Equation (18) this implies that

$$\left| \frac{\partial \rho\omega}{\partial x} \right| \quad \text{and} \quad \left| \frac{\partial (\rho_\eta U)}{\partial x} \right|$$

must be small if extrapolation is to be used.

BOUNDARY CONDITIONS FOR THE NAVIER-STOKES EQUATIONS

The 2-D Navier-Stokes equations are

$$\frac{\partial \rho U_i}{\partial x_i} = 0 \tag{1}$$

$$\frac{\partial \rho U_i U_j}{\partial x_j} = - \frac{\partial p}{\partial x_j} + \frac{\partial}{\partial x_j} (\tau_{ij}) \tag{2}$$

$$\frac{\partial \rho (U_j h)}{\partial x_j} = U_j \frac{\partial p}{\partial x_j} + \frac{\partial}{\partial x_j} \left(k \frac{\partial T}{\partial x_j}\right) + \tau_{ij}\varepsilon_{ij} \tag{3}$$

where

$$\tau_{ij} = 2\mu\varepsilon_{ij} - \mu(\partial U_k/\partial x_k)\delta_{ij} \tag{4}$$

$$\varepsilon_{ij} = 1/2 \left(\frac{\partial U_i}{\partial x_j} + \frac{\partial U_j}{\partial x_i}\right) \tag{5}$$

μ is the coefficient of viscosity and k is the coefficient of thermal conductivity.

If the thermal conductivity is neglected (i.e., k = 0), then Equation (3) can be written as

$$\rho U_j \frac{\partial h}{\partial x_j} = U_j \frac{\partial p}{\partial x_j} + \tau_{ij}\varepsilon_{ij} \tag{6}$$

Equation (2) can be written as

$$\rho U_j \frac{\partial U_i}{\partial x_j} = - \frac{\partial p}{\partial x_j} + \frac{\partial}{\partial x_j} (\tau_{ij}) \tag{7}$$

or

$$\left.\begin{aligned} \rho U \frac{\partial U}{\partial x} + \rho V \frac{\partial U}{\partial y} &= - \frac{\partial p}{\partial x} + \frac{\partial}{\partial y} \tau_{12} + \frac{\partial}{\partial x} \tau_{11} \\ \rho U \frac{\partial V}{\partial x} + \rho V \frac{\partial V}{\partial y} &= - \frac{\partial p}{\partial y} + \frac{\partial}{\partial x} \tau_{21} + \frac{\partial}{\partial y} \tau_{22} \end{aligned}\right\} \tag{8}$$

Equation (8) can be written as

$$\left.\begin{aligned} \rho \frac{\partial U^2/2}{\partial x} + \rho V \left(\frac{\partial U}{\partial y} - \frac{\partial V}{\partial x}\right) + \rho \frac{\partial V^2/2}{\partial x} &= - \frac{\partial p}{\partial x} + \frac{\partial}{\partial y} \tau_{12} + \frac{\partial}{\partial x} \tau_{11} \\ - \rho U \left(\frac{\partial U}{\partial y} - \frac{\partial V}{\partial x}\right) + \rho \frac{\partial}{\partial y} (U^2/2) + \rho \frac{\partial V^2/2}{\partial y} &= - \frac{\partial p}{\partial y} + \frac{\partial}{\partial x} \tau_{21} + \frac{\partial}{\partial y} \tau_{22} \end{aligned}\right\} \tag{9}$$

Equation (9) can be written in terms of the vorticity, ω, as

$$\left.\begin{aligned} \rho \frac{\partial}{\partial x} \left(\frac{1}{2} q^2\right) + \rho V \omega &= -\frac{\partial p}{\partial x} + \frac{\partial}{\partial x} \tau_{11} + \frac{\partial}{\partial y} \tau_{12} \\ \rho \frac{\partial}{\partial y} \left(\frac{1}{2} q^2\right) - \rho U \omega &= -\frac{\partial p}{\partial y} + \frac{\partial}{\partial x} \tau_{21} + \frac{\partial}{\partial y} \tau_{22} \end{aligned}\right\} \tag{10}$$

Using Gibbs relation,

$$Tds = dh - \frac{1}{\rho}dp \tag{11}$$

Equation (10) can be written as

$$\left.\begin{aligned} \frac{\partial}{\partial x}\left(\frac{1}{2}q^2\right) + V\omega &= T\frac{\partial s}{\partial x} - \frac{\partial h}{\partial x} + \frac{1}{\rho}\frac{\partial}{\partial x}\tau_{11} + \frac{1}{\rho}\frac{\partial}{\partial y}\tau_{12} \\ \frac{\partial}{\partial y}\left(\frac{1}{2}q^2\right) - U\omega &= T\frac{\partial s}{\partial y} - \frac{\partial h}{\partial y} + \frac{1}{\rho}\frac{\partial}{\partial y}\tau_{22} + \frac{1}{\rho}\frac{\partial}{\partial x}\tau_{21} \end{aligned}\right\} \tag{12}$$

In general,

$$2UV\omega = T\left\{U\frac{\partial s}{\partial x} - V\frac{\partial s}{\partial y}\right\} - U\frac{\partial H}{\partial x} + V\frac{\partial H}{\partial y} + \frac{U}{\rho}\left(\frac{\partial \tau_{11}}{\partial x} + \frac{\partial \tau_{12}}{\partial y}\right) - \frac{V}{\rho}\left(\frac{\partial \tau_{22}}{\partial y} + \frac{\partial \tau_{21}}{\partial x}\right) \tag{13}$$

where

$$H = h + \tfrac{1}{2}q^2 \tag{14}$$

since by definition

$$U_j\frac{\partial H}{\partial x_j} = U_j\frac{\partial h}{\partial x_j} + U_j\frac{\partial \frac{1}{2}q^2}{\partial x_j} \tag{15}$$

then, on using the energy equation, Equation (6) becomes

$$U_j\frac{\partial H}{\partial x_j} = \frac{1}{\rho}U_j\frac{\partial p}{\partial x_j} + U_j\frac{\partial \frac{1}{2}q^2}{\partial x_j} + \frac{1}{\rho}\tau_{ij}\varepsilon_{ij} \tag{16}$$

Note that the highest derivative of U_i in Equation (16) is a first derivative.

The basic equation for the stream function is

$$\nabla^2\psi = \rho\omega + \rho_y U - \rho_x V \tag{17}$$

and from Equations (13) and (16) it is clear that the highest derivative of the velocity in Equation (17) comes from the term connected with $\rho\omega$, through

$$\frac{1}{V}\left(\frac{\partial \tau_{1j}}{\partial x_j}\right) - \frac{1}{U}\left(\frac{\partial \tau_{2j}}{\partial x_j}\right)$$

Now from Equations (4) and (5)

$$\tau_{ij} = \mu\left(\frac{\partial U_i}{\partial x_j} + \frac{\partial U_j}{\partial x_i}\right) - \mu\frac{\partial U_k}{\partial x_k}\delta_{ij}$$

and

$$\frac{\partial \tau_{ij}}{\partial x_j} = \mu\left(\frac{\partial^2 U_i}{\partial x_j \partial x_j} + \frac{\partial^2 U_j}{\partial x_i \partial x_j}\right) - \mu\frac{\partial^2 U_k \delta_{ij}}{\partial x_k \partial x_j}$$

and, thus

$$U\frac{\partial \tau_{1j}}{\partial x_j} - V\frac{\partial \tau_{2j}}{\partial x_j} = \mu\,(U\,U_{yy} - V\,V_{xx} + U\,U_{xx} - V\,V_{yy}) \qquad (18)$$

and hence the highest derivative terms in Equation (17) are given by

$$\mu\left(\frac{U_{yy}}{V} + \frac{U_{xx}}{V} - \frac{V_{xx}}{U} - \frac{V_{yy}}{U}\right)$$

If a stream function ψ is defined such that

$$\rho U = \psi_y,\ \rho V = -\psi_x, \qquad (19)$$

then Equation (17) can be written as

$$U\nabla^2(\psi_y) + V\nabla^2(\psi_x) = F(\psi_x, \psi_y, \rho, S, T) \qquad (20)$$

where F contains lower derivatives than the third. Equation (20) can be written as

$$\nabla^2\bar{\psi} = f \qquad (21)$$

where

$$\bar{\psi} = -\psi_x^2 + \psi_y^2 \qquad (22)$$

Equation (21) is a Poisson equation and requires either $\overline{\psi}$ or the partial derivative of $\overline{\psi}$ be specified, i.e.,

$$\overline{\psi}_x \text{ or } \overline{\psi}_y \text{ is to be specified}$$

If $\overline{\psi}$ is specified then

$$-\psi_x^2 + \psi_y^2$$

is specified which is a combination of ρU and ρV. To solve for ψ the differential Equation (22) must be solved; this requires that ψ or one of its derivatives be specified. Thus to solve Equation (21) two of the boundary conditions are that ρU and ρV be specified.

Now from Equations (1) and (2)

$$\rho U_j U_i \frac{\partial U_i}{\partial x_j} = -U_i \frac{\partial p}{\partial x_i} + U_i \frac{\partial \tau_{ij}}{\partial x_j} \tag{23}$$

Thus from Equations (6), (23), and (14)

$$\rho U_j \frac{\partial h}{\partial x_j} = \rho U_j \frac{\partial H}{\partial x_j} + U_i \frac{\partial p}{\partial x_i} - U_i \frac{\partial \tau_{ij}}{\partial x_j} = U_j \frac{\partial p}{\partial x_j} + \tau_{ij} \varepsilon_{ij} \tag{24}$$

or

$$\begin{aligned} \rho U_j \frac{\partial H}{\partial x_j} &= \frac{1}{2} \tau_{ij} \left(\frac{\partial U_i}{\partial x_j} + \frac{\partial U_j}{\partial x_i}\right) + U_i \frac{\partial \tau_{ij}}{\partial x_j} \\ &= \frac{1}{2} \tau_{ij} \left(\frac{\partial U_j}{\partial x_i} + \frac{\partial U_i}{\partial x_j}\right) + \frac{\partial (\tau_{ij} U_i)}{\partial x_j} - \tau_{ij} \frac{\partial U_i}{\partial x_j} \qquad (25) \\ &= \frac{1}{2} \tau_{ij} \left(\frac{\partial U_j}{\partial x_i} - \frac{\partial U_i}{\partial x_j}\right) + \frac{\partial (\tau_{ij} U_i)}{\partial x_j} \end{aligned}$$

Using Equation (4)

$$\tau_{ij} \left(\frac{\partial U_j}{\partial x_i} - \frac{\partial U_i}{\partial x_j}\right) = \left[\mu \left(\frac{\partial U_i}{\partial x_j} + \frac{\partial U_j}{\partial x_i}\right) - \mu \delta_{ij} \frac{\partial U_k}{\partial x_k} \right] \left(\frac{\partial U_j}{\partial x_i} - \frac{\partial U_i}{\partial x_j}\right) \tag{26}$$

or

$$\tau_{ij}\left(\frac{\partial U_j}{\partial x_i} - \frac{\partial U_i}{\partial x_j}\right) = \mu\left\{\frac{-\partial U_i}{\partial x_j}\frac{\partial U_i}{\partial x_j} + \frac{\partial U_j}{\partial x_i}\frac{\partial U_j}{\partial x_i}\right\} = 0 \qquad (27)$$

Hence, on using continuity (Equation (1)), Equation (25) gives

$$\frac{\partial}{\partial x_j}(\rho U_j H) = \frac{\partial}{\partial x_j}(\tau_{ij} U_i) \qquad (28)$$

An alternative version is

$$\frac{\partial}{\partial x_j}(\rho U_j H) = \frac{\partial}{\partial x_j}(\tau_{ij} u_i) + H_o \frac{\partial \rho u_j}{\partial x_j} \qquad (29)$$

or

$$\rho U_j (H - H_o) = \tau_{ij} U_i \qquad (30)$$

so that if H_o is the stagnation value of H, Equation (30) is consistent.

Multiplication of Equation (30) by U_j and using Equations (4) and (5) gives

$$\rho q^2 (H - H_o) = \mu\left\{U_i U_j\left(\frac{\partial U_i}{\partial x_j} + \frac{\partial U_j}{\partial x_i}\right) - \delta_{ij}\frac{\partial U_k}{\partial x_k} U_i U_j\right\} \qquad (31)$$

or

$$\begin{aligned}\rho q^2 (H - H_o) &= \mu\left\{U_j \frac{\partial q^2/2}{\partial x_j} + U_i \frac{\partial q^2/2}{\partial x_i} - q^2 \frac{\partial U_k}{\partial x_k}\right\} \\ &= \mu\left\{U_j \frac{\partial q^2}{\partial x_j} - q^2 \frac{\partial U_k}{\partial x_k}\right\}\end{aligned} \qquad (32)$$

Equation (32) can be manipulated to give

$$C_p \rho T + \frac{1}{2}\rho q^2 - C_p \rho T_o = \frac{\mu}{q^2}\left\{U_j \frac{\partial q^2}{\partial x_j} - q^2 \frac{\partial U_k}{\partial x_k}\right\} = Q \qquad (33)$$

From Gibbs relation and the gas law

$$\left(\frac{p}{p_\infty}\right) \Big/ \left(\frac{\rho}{\rho_\infty}\right)^{\gamma} = \exp\ (S/C_v) \qquad (34)$$

then

$$C_p\ \rho T = C_p\ \frac{p}{R}_\infty = \frac{\gamma}{\gamma-1}\ p_\infty\ \left(\frac{\rho}{\rho}\right)^{\gamma}\ \exp\ (S/C_v) \qquad (35)$$

and Equation (33) gives

$$\exp\ (S/C_v)\ \left(\frac{\gamma}{\gamma-1}\right)\ p_\infty\ \left(\frac{\rho}{\rho_\infty}\right)^{\gamma} + \rho_\infty\ \left(\frac{\rho}{\rho_\infty}\right)\ \left(\frac{1}{2}\ q^2 - C_p T_o\right) = Q \qquad (36)$$

which is an equation for ρ in terms of Q, S, ρ_∞, and p_∞. If U_j (and hence Q) is specified on the boundary and if S is known, then ρ, p, and T (and consequently h) can be found from Equations (34), (36), and the gas equation. In general, S, p, or T must be specified on the boundary and the other thermodynamic variables are given in terms of this variable and ρ. The boundary conditions for the steady Navier-Stokes equations are therefore

(a) ρU, ρV specified on a boundary
(b) S, p, or T specified on a boundary
(c) ρ_∞, p_∞ specified as a datum

REFERENCES

1. Yee, H. C.: Numerical Approximation of Boundary Conditions with Applications to Inviscid Equations of Gas Dynamics. NASA Tech. Mem. 81265, 1981.

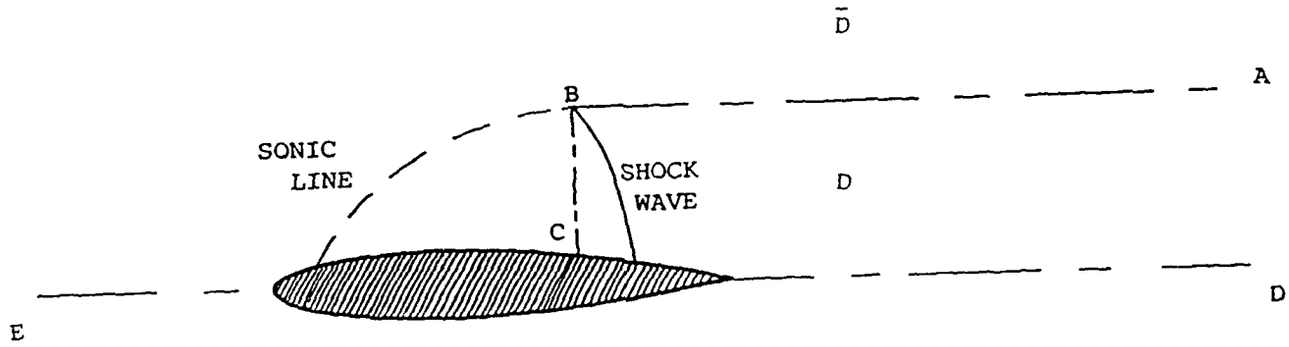

FIGURE 1.

APPENDIX B

The Application of Nonreflecting Boundary Conditions to 2-D Unsteady Computations on Curvilinear Grids

SUMMARY

The ability to apply flow-through boundary conditions in places where the flowfield is neither steady nor uniform would allow CFD computations over smaller domains, thus requiring fewer grid points. Recently, nonreflecting boundary conditions have received a lot of attention as a promising method for specifying outflow boundary conditions on a shortened domain.[1-3] Nonreflecting boundary conditions have been derived by Thompson[1] for the Euler equations in Cartesian and spherical coordinates. This work extends Thompson's formulation to curvilinear coordinates, so that it may be applied to practical two-dimensional CFD problems. The theory is valid for hyperbolic, quasi one-dimensional flows, but loses accuracy and stability for computations of low subsonic flows with strong two-dimensionality. This loss of accuracy is demonstrated for the problem of subsonic vortex shedding through a boundary.

INTRODUCTION

Most computational fluid dynamics (CFD) problems are solved assuming that the solution domain boundaries are either in a uniform stream or at a solid surface. For boundaries in a uniform freestream, which is at a known velocity and angle of attack, boundary conditions derived from one-dimensional characteristic theory can be applied in a relatively straightforward manner. However, it is of practical importance to be able to apply boundary conditions in locations where there are flow gradients present, or where the flow is unsteady. For example, many flows have a wake structure which persists for a long distance downstream, and it is too computationally expensive to have a solution domain extend to where uniform flow conditions may be applied.

Nonreflecting boundary conditions have been developed as a promising means of applying boundary conditions at an outflow.[1-3] These boundary conditions prevent the reflections of outgoing waves back into the computational domain and also eliminate incoming waves, which are unknown since they originate from outside the domain. However, these boundary conditions are only accurate for a limited subclass of flow fields. For instance, Thompson[1] noted that these boundary conditions will be inaccurate for problems where the flow should be influenced by incoming waves, and Watson and Myers[2] found that the formulation used for these boundary conditions is unstable for nonplanar acoustic sources at an inflow. Other errors may occur in viscous subsonic flow computations, as the boundary conditions are derived from the hyperbolic Euler equations.

Although some errors may be expected, nonreflecting boundary conditions provide one of the few options currently available for treating the outflow of unsteady nonuniform flows. Therefore, it is necessary to investigate the suitability of these boundary conditions for practical flow problems, to determine whether any errors involved are within a tolerable range. This paper investigates the application of nonreflecting boundary conditions to subsonic flows with a wake structure that passes through the outflow boundary.

DERIVATION OF CURVILINEAR BOUNDARY CONDITIONS

The vast majority of Euler and Navier-Stokes finite difference computations for aeronautical applications take place on curvilinear grids, in order to allow for realistic geometries. The first stage of this work was to extend Thompson's[1] formulation of nonreflecting boundary conditions to the general curvilinear case. This work was completed for boundaries in both the curvilinear coordinate directions.

The first step was to write the Euler equations in primitive variable form and then to group together the spatial derivatives which are normal to the computational boundary. These derivatives will eventually be rewritten to represent the nonreflecting condition, while the spatial derivatives tangential to the boundary will be left unaltered.

Let x and y represent the Cartesian coordinate variables and ξ and η represent the curvilinear coordinate variables. For a problem where the outflow boundary runs along an η=constant gridline, the terms in the Euler equations involving η-derivatives are to be rewritten. The Euler equations are placed in characteristic form, so that the eigenvalues are given explicitly. The characteristic terms for the η-derivatives are given by:

$$M1 = \left[V - c\sqrt{\eta_x^2 + \eta_y^2} \right] \left(p_\eta - \rho c \tilde{\eta}_x u_\eta - \rho c \tilde{\eta}_y v_\eta \right)$$

$$M2 = V \left(p_\eta - c^2 \rho_\eta \right)$$

$$M3 = V \left(\tilde{\eta}_y u_\eta - \tilde{\eta}_x v_\eta \right)$$

$$M4 = \left[V + c\sqrt{\eta_x^2 + \eta_y^2} \right] \left(p_\eta + \rho c \tilde{\eta}_x u_\eta + \rho c \tilde{\eta}_y v_\eta \right)$$

where $\tilde{\eta}_x = \eta_x \Big/ \sqrt{\eta_x^2 + \eta_y^2}$

$$\tilde{\eta}_y = \eta_y \Big/ \sqrt{\eta_x^2 + \eta_y^2}$$

let $\alpha = \sqrt{\eta_x^2 + \eta_y^2}$

u and v are the velocities along x and y, U and V are the contravariant velocities along ξ and η, and c is the speed of sound. This formulation of the characteristic equations assumed

quasi one-dimensional flow, that is, the derivatives with respect to ξ and η are separable, and the cross-terms are neglected.

For a subsonic outflow boundary, M1 represents incoming waves, and M2 - M4 represent outgoing waves. In the Euler equations, the η-derivative terms are written in terms of M1 - M4. Then, at the boundary, M1 is set equal to zero, and M2 - M4 are computed numerically. The equations are written in conservative form and are solved together with the interior equations. The final form of the Euler equations at the boundary is

$$\frac{\partial \bar{Q}}{\partial \tau} + \xi_t \frac{\partial \bar{Q}}{\partial \xi} + \xi_x \frac{\partial \bar{E}}{\partial \xi} + \xi_y \frac{\partial \bar{F}}{\partial \xi} - T \frac{\partial Q}{\partial \eta} = 0$$

where $\bar{Q} = \begin{bmatrix} \rho \\ \rho u \\ \rho v \\ e \end{bmatrix}$ $\bar{E} = \begin{bmatrix} \rho u \\ \rho u^2 + p \\ \rho uv \\ u(e + p) \end{bmatrix}$ $\bar{F} = \begin{bmatrix} \rho v \\ \rho uv \\ \rho v^2 + p \\ v(e + p) \end{bmatrix}$

$$Q = \begin{bmatrix} \rho \\ u \\ v \\ p \end{bmatrix}$$

and T is a 4 x 4 matrix made up of the following terms:

$T_{11} = V$

$T_{12} = (V + c\alpha)\rho\bar{\eta}_x/(2c)$

$T_{13} = (V + c\alpha)\rho\bar{\eta}_y/(2c)$

$T_{14} = -(V - c\alpha)/(2c^2)$

$T_{21} = uV$

$T_{22} = \rho V + (V + c\alpha)\rho u\bar{\eta}_x/(2c)$

$T_{23} = (V + c\alpha)\rho u\bar{\eta}_y/(2c)$

$T_{24} = -(V - c\alpha)u/(2c^2) + \eta_x$

$T_{31} = vV$

$T_{32} = (V + c\alpha)\rho v\bar{\eta}_x/(2c) - (V - c\alpha)\rho\eta_x/(2\eta_y)$

$T_{33} = (V + c\alpha)(\rho/2 + \rho v\bar{\eta}_y/(2c))$

$$T_{34} = (V + c\alpha)/(2c\tilde{\eta}_y) - (V - c\alpha)/(2c^2) - \eta_x^2/\eta_y$$

$$T_{41} = V(u^2 + v^2)/2$$

$$T_{42} = (V + c\alpha)(u^2 + v^2)\rho\tilde{\eta}_x/(4c) + (V + c\alpha)\rho c\tilde{\eta}_x/(2\gamma - 2) - (V - c\alpha)\rho v\eta_x/(2\eta_y) + \rho V$$

$$T_{43} = (V + c\alpha)(u^2 + v^2)\rho\tilde{\eta}_y/(4c) + (V + c\alpha)\rho v/2 + (V + c\alpha)\rho c\tilde{\eta}_y/(2\gamma - 2)$$

$$T_{44} = -(V - c\alpha)(u^2 + v^2)/(4c^2) - (V + c\alpha)v/(2c\tilde{\eta}_y) + (V + c\alpha)/(2\gamma - 2) + u\eta_x - v\eta_x^2/\eta_y$$

The corresponding equations for a boundary along a ξ=constant gridline have also been derived in this work. Those results will be published in the future.

The solution of the boundary equations was made using the same algorithm as the interior equations. The numerical algorithm is a block tridiagonal implicit method using Beam-Warming second-order time differencing.

RESULTS

Several test cases were run to test this formulation. The first test case was a solution over a Cartesian grid, where the curvilinear coordinate formulation reduces to the boundary conditions given by Thompson.[1] A simple one-dimensional pressure pulse was given as the initial condition, with a freestream Mach number equal to 0.1 (this insured that there was outflow only at the downstream boundary). A solution using extrapolation boundary conditions was obtained over a large domain, and the solution was stopped before the pressure pulse reached the downstream boundary. Thus, there should not have been any influence from that boundary condition in the interior. Then, a solution using the nonreflecting boundary conditions was obtained on a shortened domain, and the solution was run until the pressure wave passed through the boundary. A comparison of the two solutions gave an indication of how "transparent" the nonreflecting boundary conditions were.

The results of this test were quite satisfactory. There was little noticeable difference between the solution over the truncated domain and the full solution (Figure 1). The test was repeated with a two-dimensional pressure pulse. In this case, the results were not as good. Although the pressure wave did pass through the boundary, there was some distortion near the boundary (Figure 2). It is possible that if the cross-terms in the characteristic equations were not neglected in the formulation, the differences between the one-dimensional and two-dimensional problems would be insignificant.

These tests were repeated on a curved grid to test the curvilinear formulation. These tests gave the same results as those on the Cartesian grid (Figure 3).

The next test case was that of a single vortex passing through a boundary. The initial condition was that of a vortex velocity distribution, but with a uniform pressure and density field. The low pressure within the vortex developed shortly after the solution was begun. Again, both a solution over a long domain was found, with the calculation stopping before the vortex hit the downstream boundary, and a solution using nonreflecting boundary

conditions was found over a shortened domain. Solutions over both a Cartesian grid and a curvilinear grid gave the same results. The solution over the curvilinear grid is shown here. The freestream has a Mach number of 0.2, and contours of pressure, vorticity, and Mach number are plotted (Figures 4-6). These results show that the vorticity and the Mach number propagate through the boundary with reasonable accuracy. However, the pressure field does not pass through the boundary accurately. Instead, a distinct pressure reflection is seen, which grows with time. Since the nonreflecting boundary conditions removes the upstream influence of the part of the vortex which is downstream of the boundary, it could be expected that the pressure at the boundary would be inaccurate.

The final test case was subsonic vortex shedding behind a circular cylinder. The freestream was at Mach = 0.2, and the Reynolds number was 100. In this case, a steady stream of vortices passes through the downstream boundary. The lift coefficient history is oscillatory, as shown in Figure 7. At the beginning of the calculation, the lift on the cylinder was zero, since a symmetric separation bubble behind the cylinder was formed. It was necessary to perturb the solution to initiate the asymmetric vortex shedding. Both the global and the truncated solutions were run independently of one another but were started in identical fashions.

Once the oscillatory lift behavior was established, the two solutions differed in both frequency and amplitude. The nonreflecting boundary conditions, by removing the upstream effects of the vortex stream once it passed through the boundary, allowed a lower frequency oscillation than the full solution. The amplitude of the lift coefficient in the nonreflecting case also seemed to level off before the full solution reached a constant amplitude. In the nonreflecting case, a high pressure wave was generated at the downstream boundary, which increased the wavelength of the vortex stream. Stream function contours of the two solutions are shown in Figure 8. The elongated wake structure is evident in the truncated solution.

CONCLUSIONS

At present, nonreflecting boundary conditions present one of the few options for treating outflow boundary conditions. However, as the theory is valid only for hyperbolic equations, it is necessary to understand the inaccuracies that would result when applying them to subsonic viscous flows. In this work, it was shown that errors in the pressure at the boundary are generated, and these errors propagate into the interior solution with time. In some cases, such as vortex shedding behind a circular cylinder at low Reynolds number, the outflow boundary conditions eventually affect the entire wake structure and the pressure forces acting on the body.

REFERENCES

1. Thompson, K. W., "Time Dependent Boundary Conditions for Hyperbolic Systems," Journal of Computational Physics, Vol. 68, 1987, pp. 1-24.

2. Giles, M. B., "Nonreflecting Boundary Conditions for Euler Equation Calculations," AIAA-89-1942, AIAA 9th Computational Fluid Dynamics Conference, Buffalo, New York, June 13-15, 1989.

3. Keller, J. B., "Exact Nonreflecting Boundary Conditions," Journal of Computational Physics, Vol. 82, 1989, pp. 172-192.

4. Watson, W. and Myers, M., "Time-Dependent Inflow-Outflow Boundary Conditions for 2-D Acoustic Systems," AIAA-89-1041, AIAA 12th Aeroacoustics Conference, San Antonio, Texas, April 10-12, 1989.

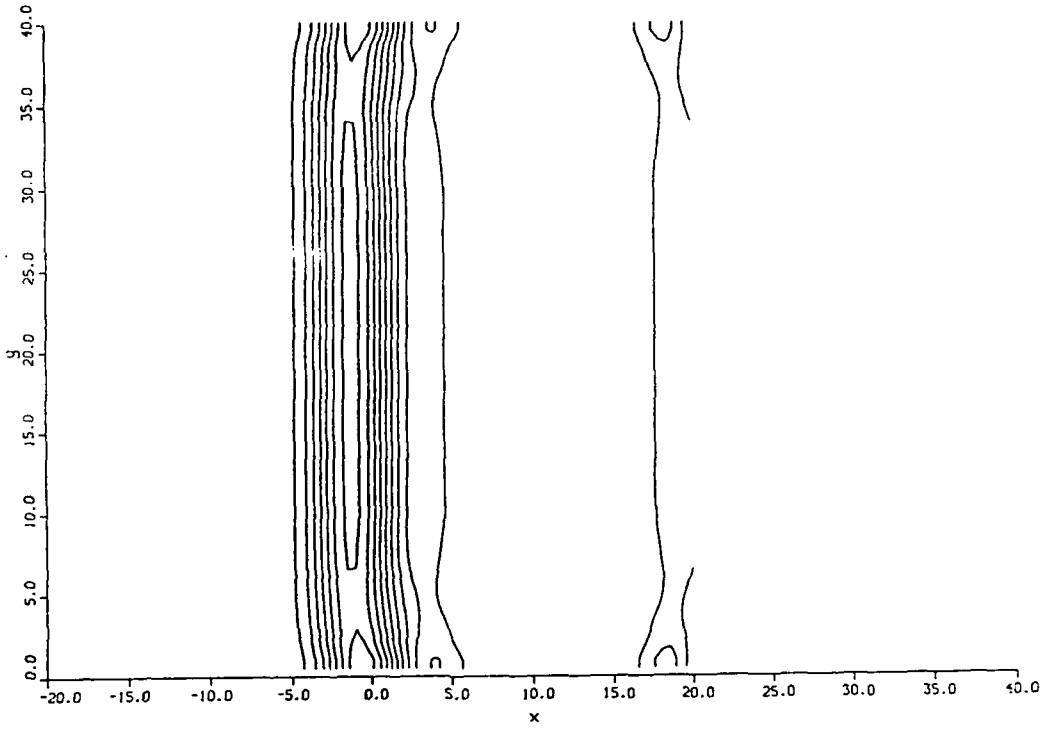

a)

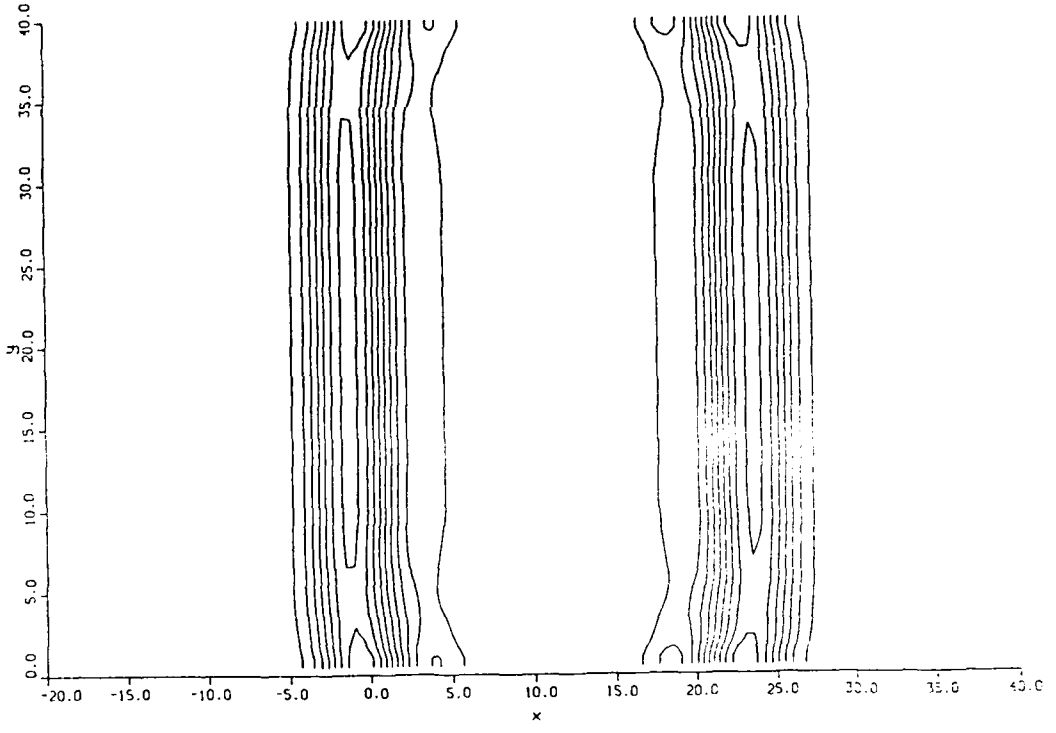

b)

Figure 1.- One-dimensional pressure pulse solution. Initial condition $P/P_\infty = 1. + 0.4 \exp(-(x-10)^2)$. a) nonreflecting boundary condition applied at x=20, b) global solution.

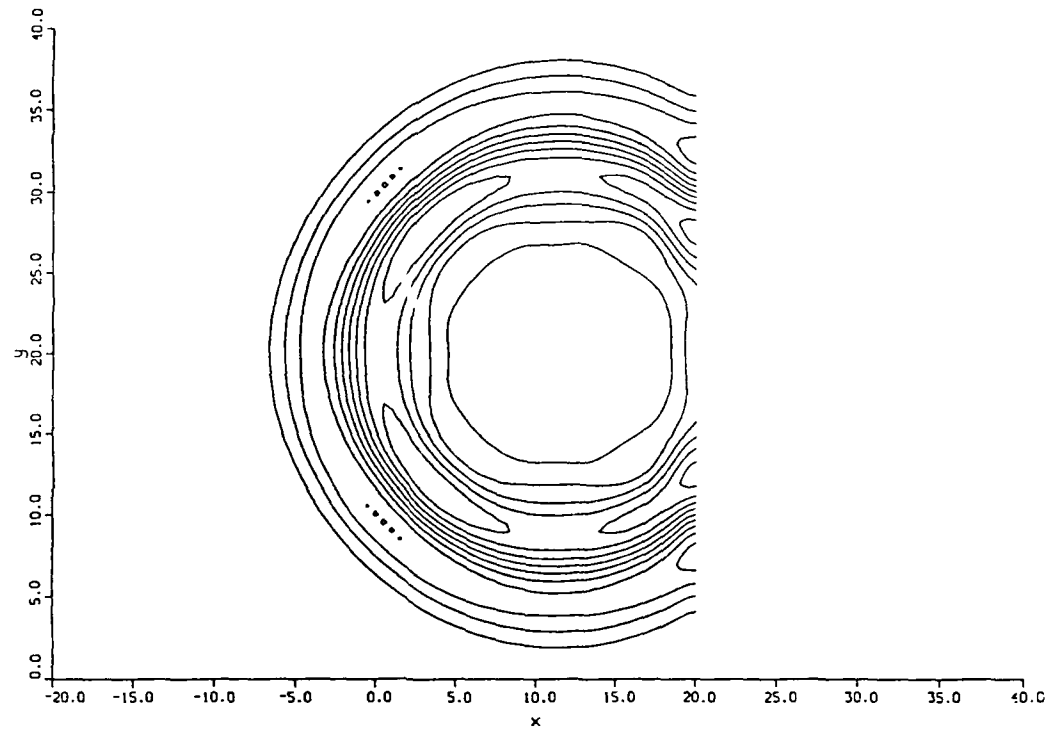

a)

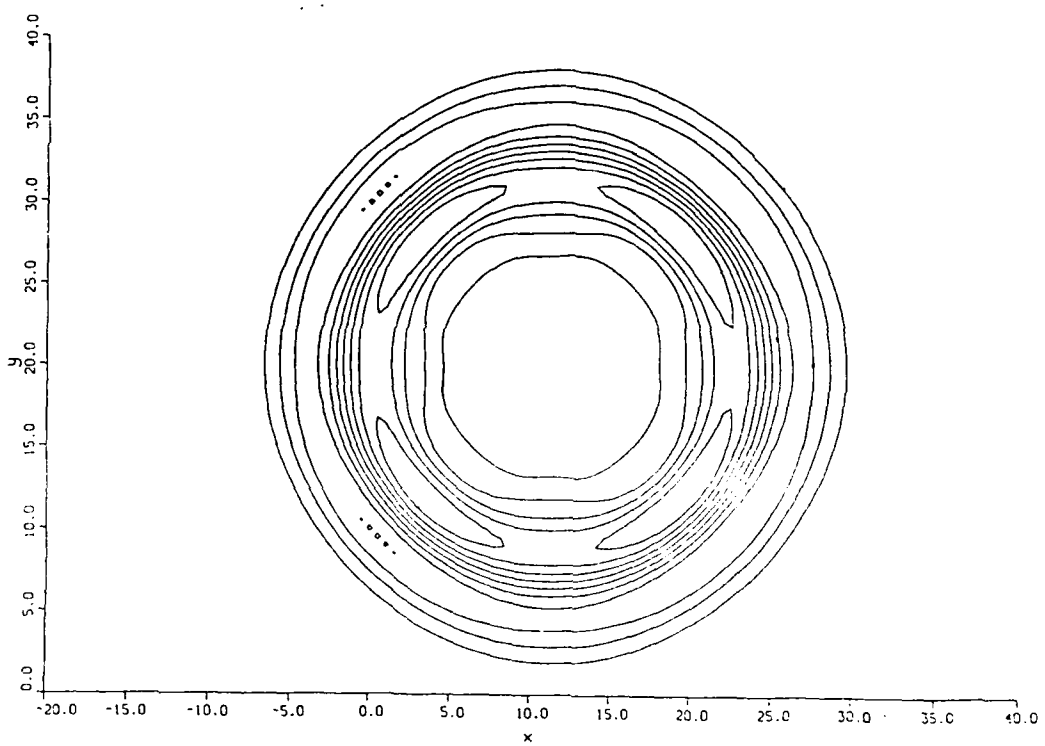

b)

Figure 2.- Two-dimensional pressure pulse solution. Initial condition $P/P_\infty = 1. + 0.4 \exp(-(x-10)^2 - (y-20)^2)$. a) nonreflecting boundary condition applied at x=20, b) global solution.

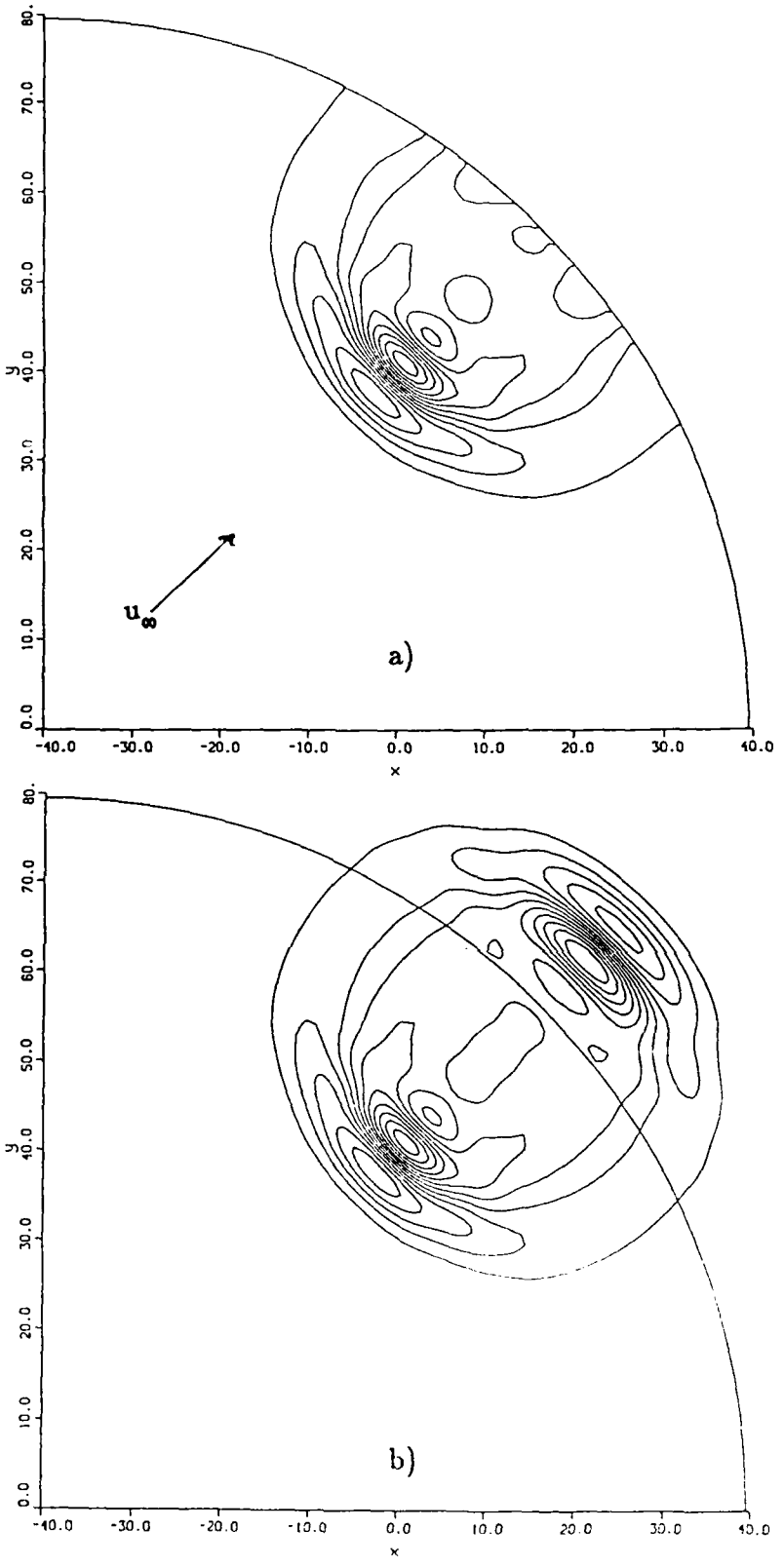

Figure 3.- Two-dimensional pressure pulse solution, same as in Figure 2 but on a curved grid. a) nonreflecting boundary condition, b) global solution.

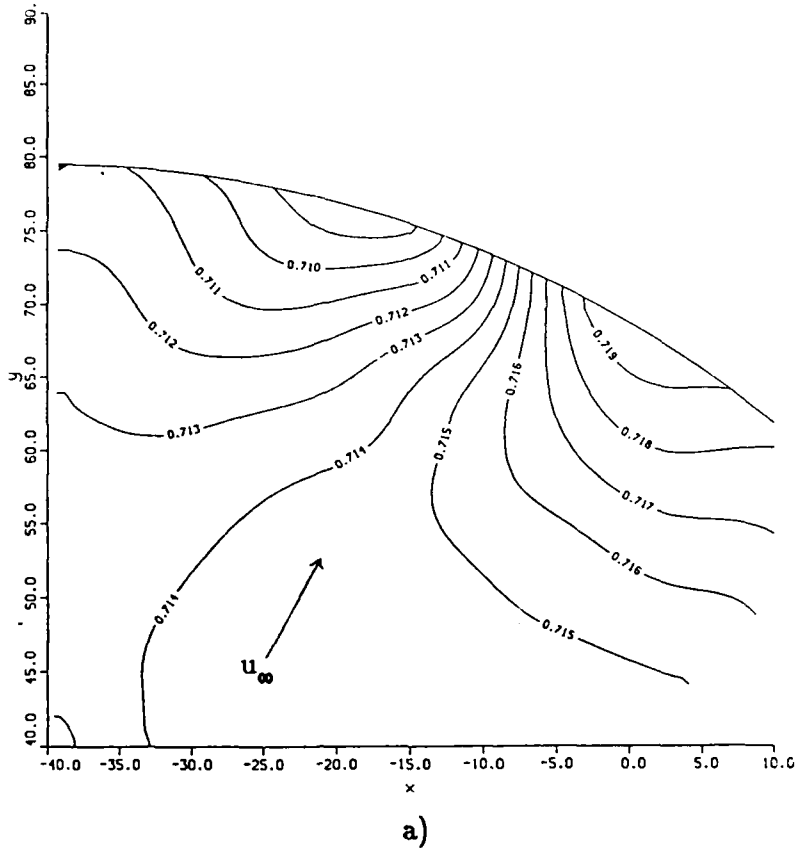

a)

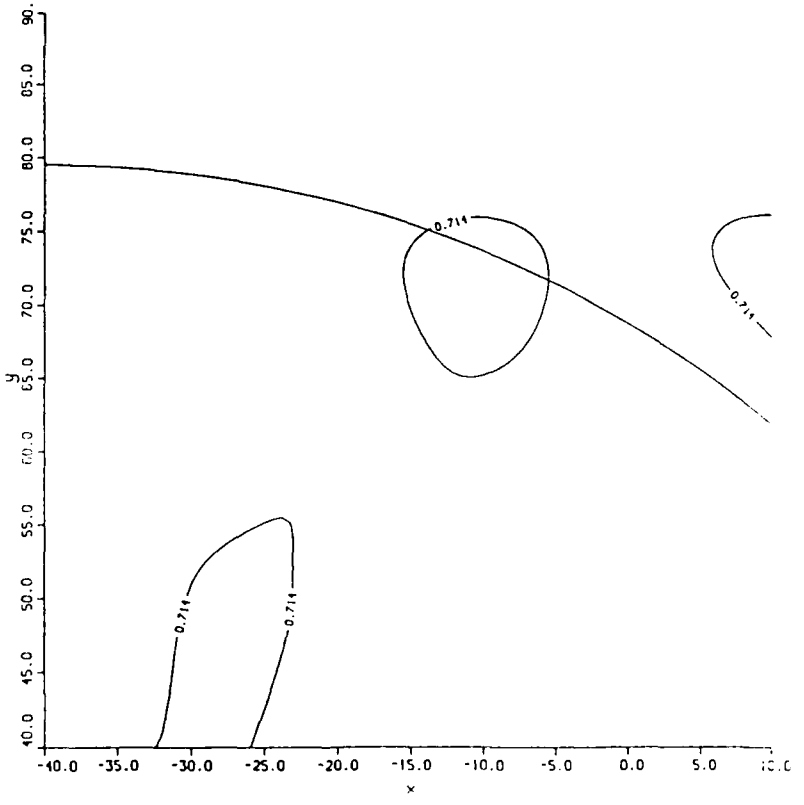

b)

Figure 4.- Single vortex pressure contours. a) nonreflecting boundary condition, b) global solution.

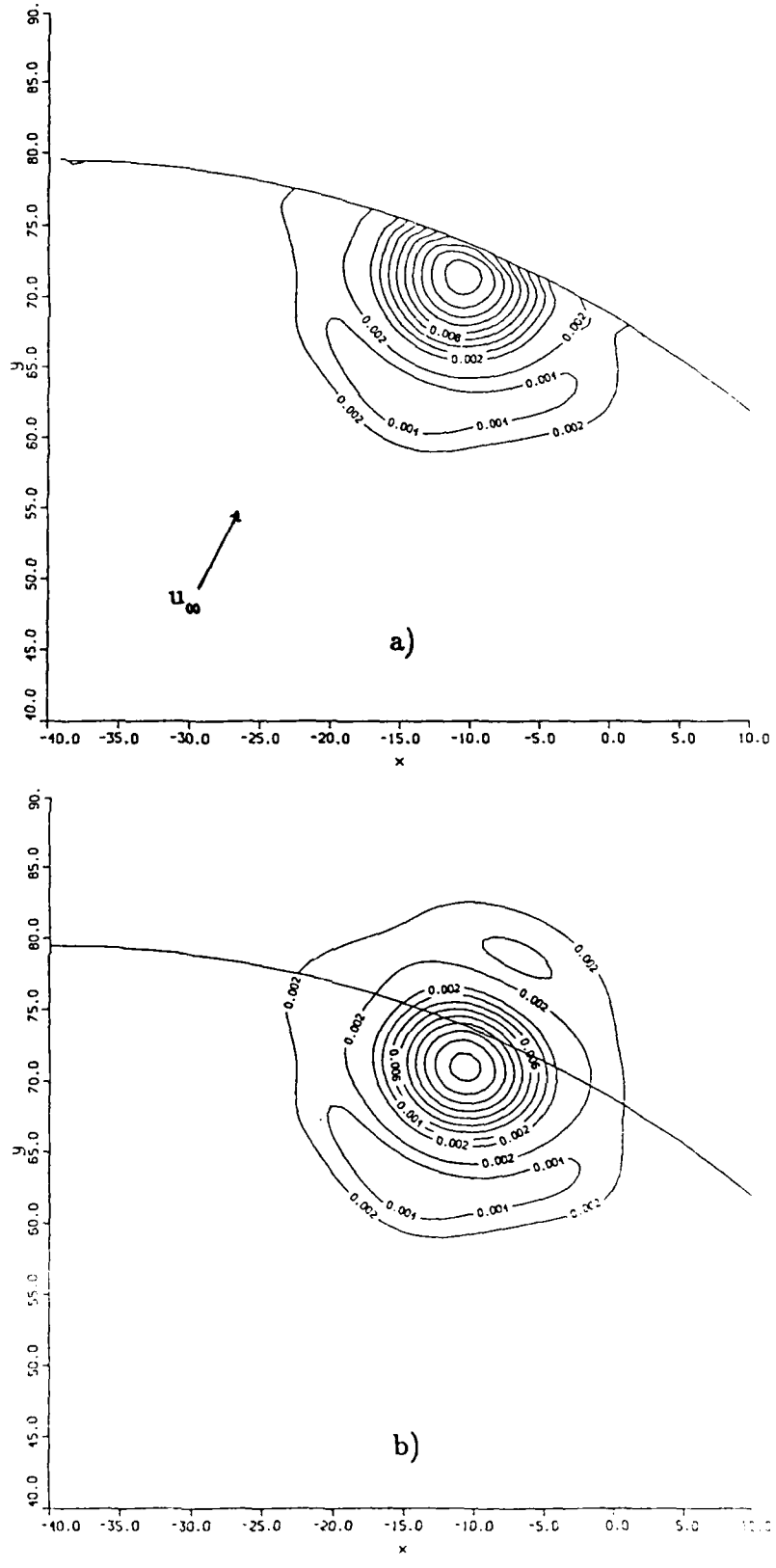

Figure 5.- Single vortex vorticity magnitude contours. a) nonreflecting boundary condition, b) global solution.

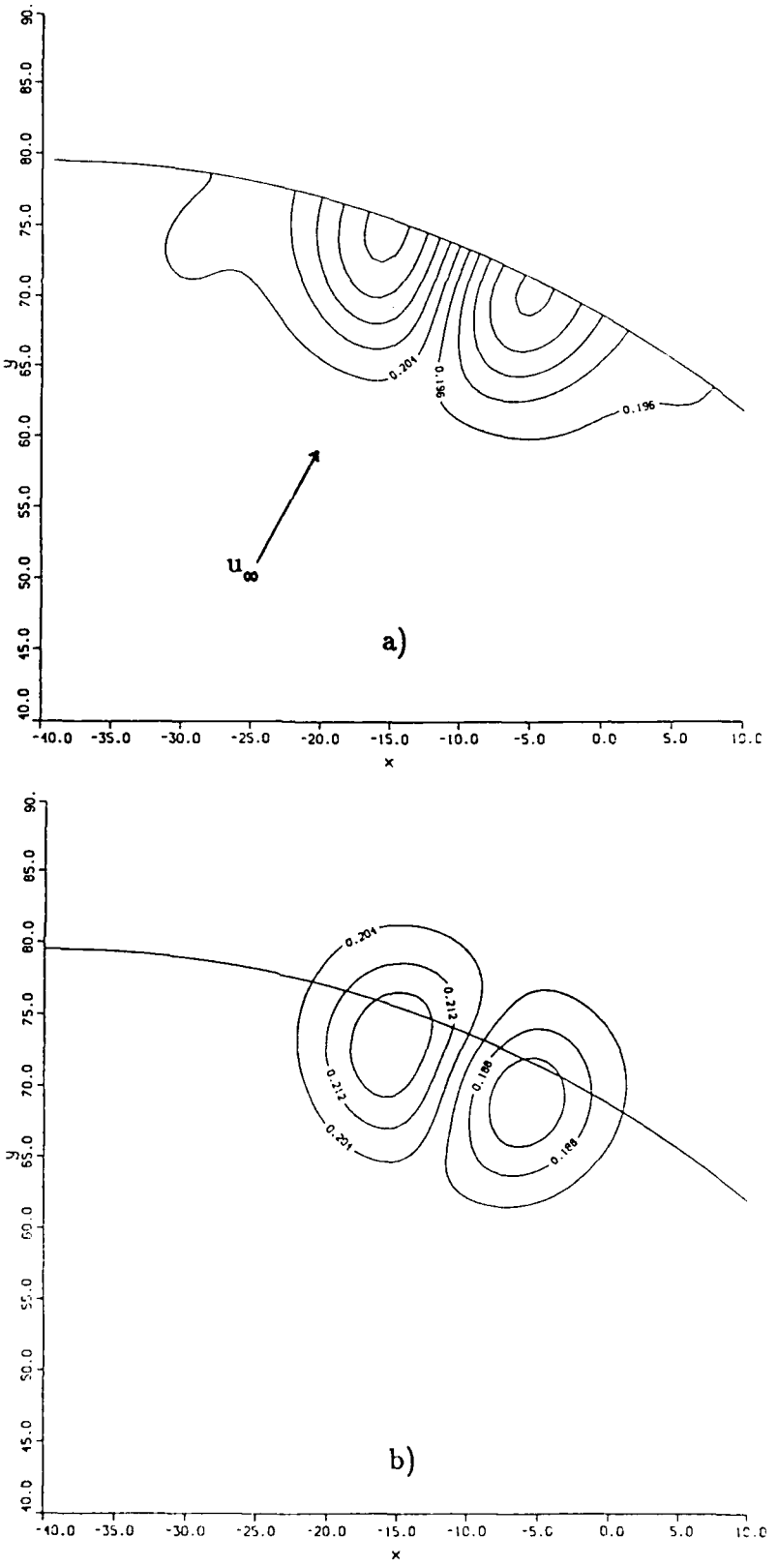

Figure 6.- Single vortex Mach number contours. a) nonreflecting boundary condition, b) global solution.

a)

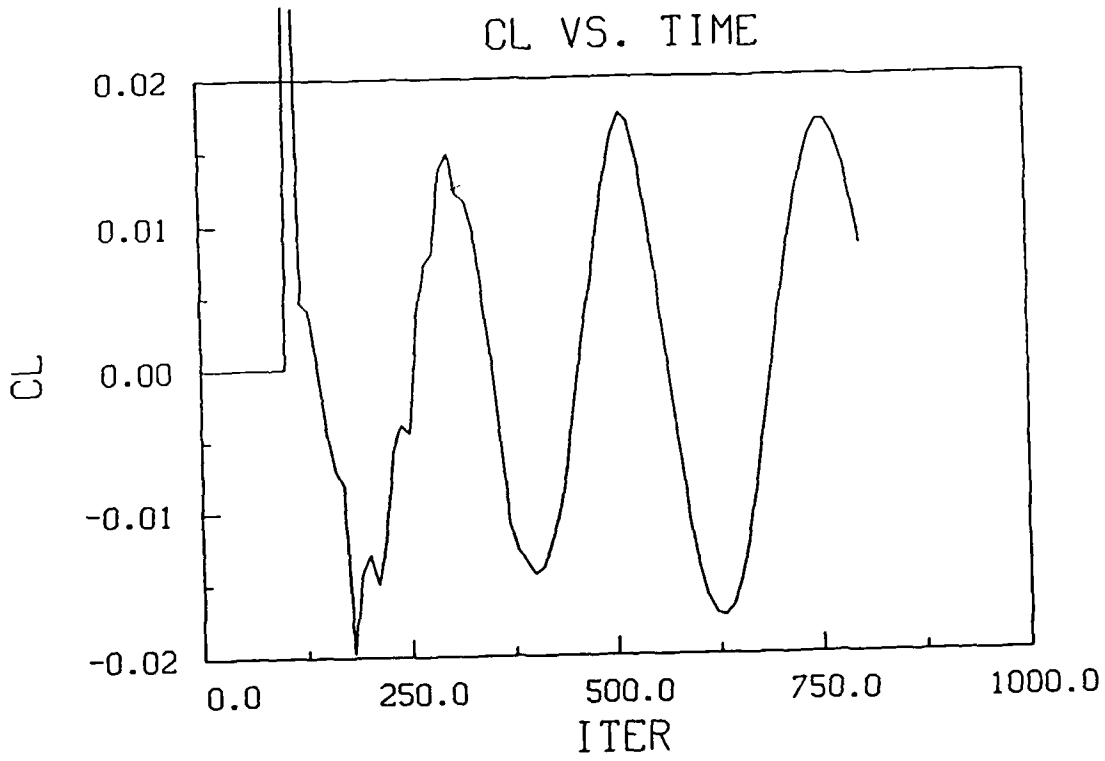

b)

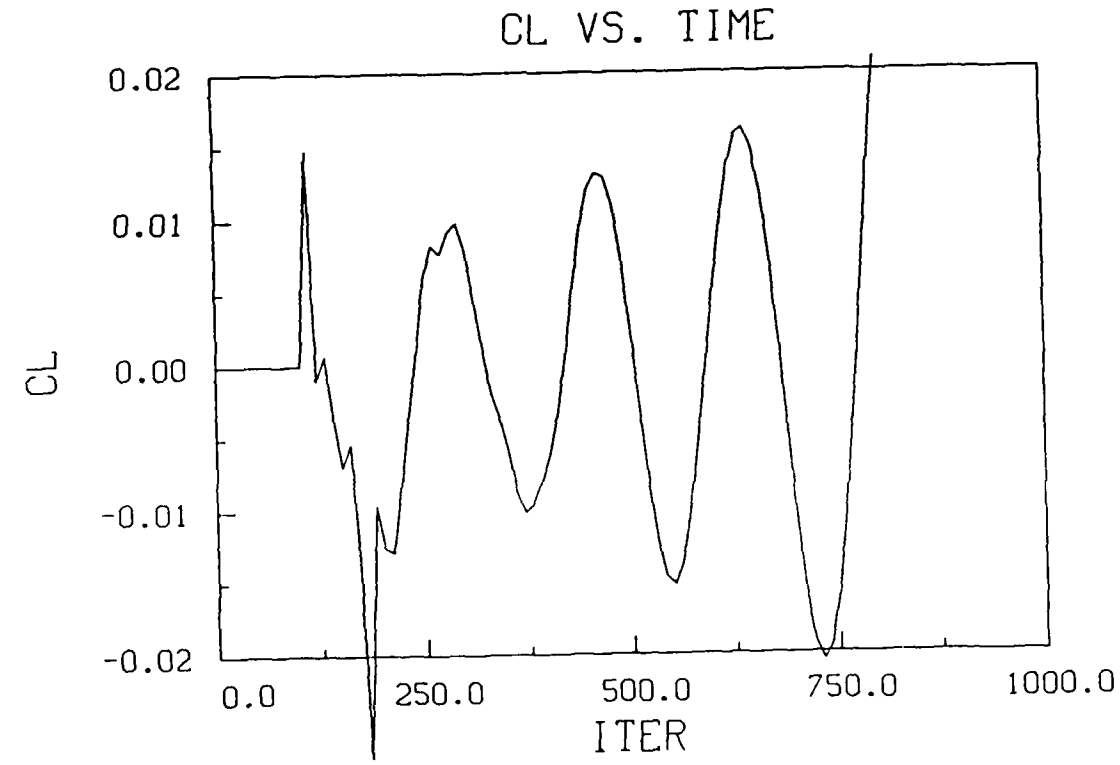

Figure 7.- Lift coefficient history for circular cylinder. a) nonreflecting boundary conditions applied 6 diameters downstream, b) global solution with boundary 16 diameters downstream. (Re=100, M=0.2)

a)

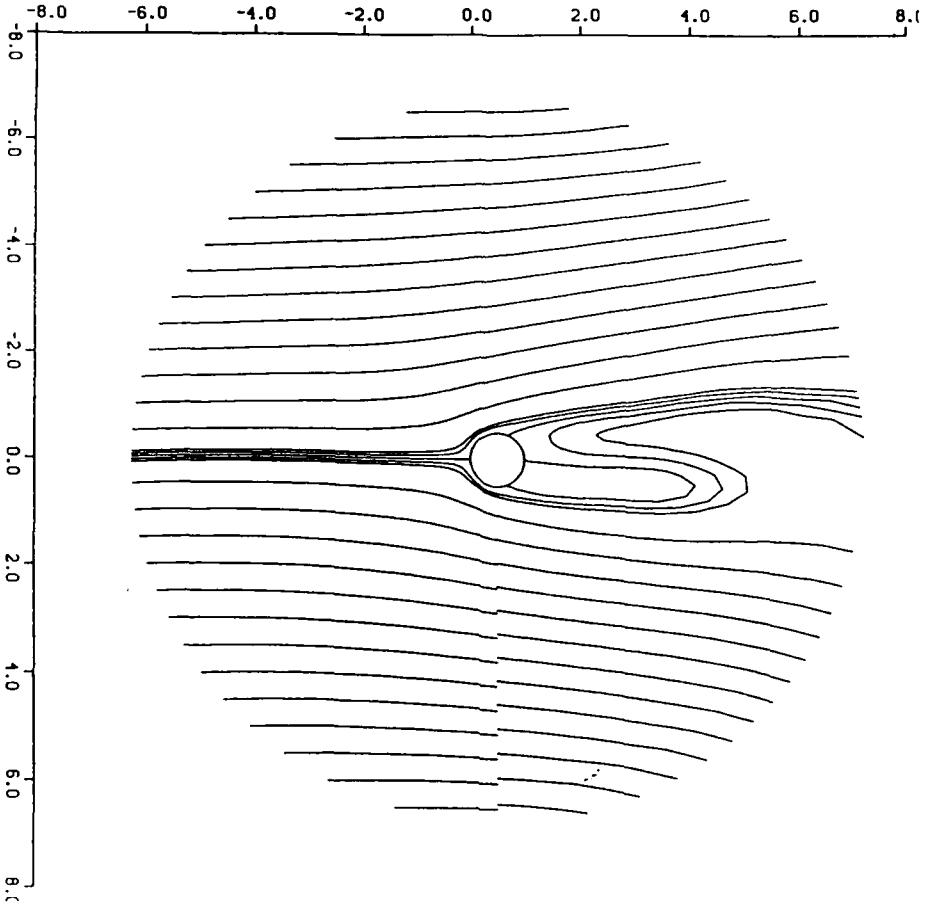

b)

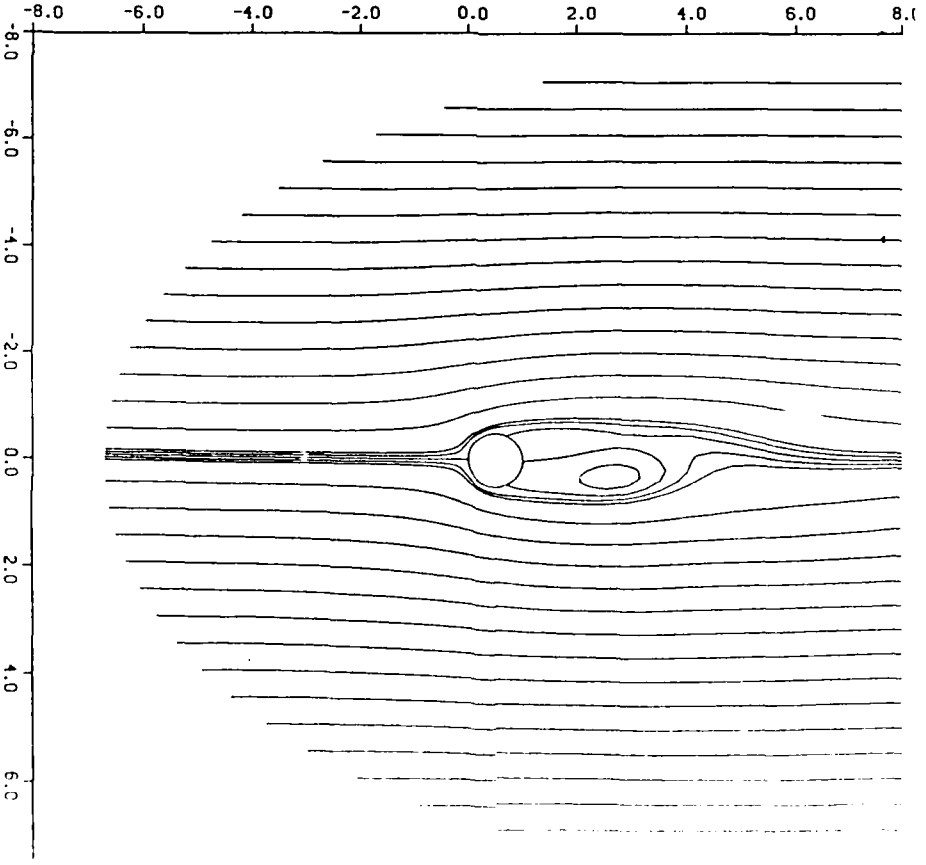

Figure 8.- Stream function contours for circular cylinder. a) nonreflecting boundary conditions applied 6 diameters downstream, b) global solution with boundary 16 diameters downstream. (Re=100, M=0.2)

APPENDIX C

Outflow Boundary Conditions for Vortex Shedding Behind a Circular Cylinder

The flow about a circular cylinder was computed in order to study the effect of outflow boundary conditions on the vortex shedding process. Since the wake for this flow persists for a large distance downstream, it is of interest to see if a boundary condition applied to a truncated domain can accurately reproduce the global flowfield. If such a boundary condition can be found, the computational efficiency of these calculations will increase greatly, as much smaller flowfield domains may be used.

The first step was to compute the global flowfield to use as a comparison to the truncated solution. The numerical procedure is described here. A two-dimensional finite difference Navier-Stokes code, ARC2D, was used, and the full viscous terms were included. The method used was an implicit second-order time-accurate Beam-Warming algorithm. Second-order central differencing of the spatial derivatives was used with the approximate factorization method. The calculation was laminar, with a Reynolds number of 100 and a Mach number of 0 1 The grid for the global solution extended twenty cylinder diameters downstream.

The boundary conditions for the global calculation were the default airfoil boundary conditions incorporated into the ARC2D flow code.[1] These boundary conditions are described here.

For the farfield inflow, as well as the top and bottom boundaries of the flow domain, the following formulation based on the one-dimensional Riemann invariants was used. Extrapolation was used to determine whether the boundary was at an inflow or an outflow. For an inflow, three variables were specified (Riemann invariant R1, the tangential velocity, and the entropy) while one variable was extrapolated from the interior (Riemann invariant R2). For an outflow, R2 was specified, and the quantities R1, the tangential velocity, and the entropy were extrapolated.

The Riemann invariants R1 and R2 are given by:

$$R1 = Q_n - 2.*a/(\gamma-1.)$$

and

$$R2 = Q_n + 2.*a/(\gamma-1.),$$

with the entropy given by ρ^{γ}/p,

where Q_n is the velocity normal to the boundary, a is the speed of sound, ρ is the density, and p is the pressure. For this problem, the specified velocities were u = 0.1 and v = 0.0 (based on speed of sound). The freestream pressure is given by $1/\gamma$, and the speed of sound is 1.0.

On the cylinder surface, the velocities were set equal to zero, and the pressure is found from the normal momentum equation. An adiabatic wall was assumed, and the density was extrapolated from the interior. For this global calculation, the outflow boundary conditions were all found from an extrapolation from the interior. These boundary conditions were applied at $x = 20$.

The grid used for this calculation was a C-type mesh, with dimensions 245x40. The grid extended from $-5 < x < 20$ and $-5 < y < 5$. The cylinder had unit diameter and was centered at the origin. The minimum normal spacing for the grid was 0.016.

The truncated solution used the identical grid up to $x = 4$. For this solution, nonreflecting boundary conditions were used.[2] As the grid used in this work was curvilinear, the analysis for Cartesian coordinates given in Reference 2 was rederived in this work for curvilinear grids. The following results are included here: both the full and truncated grids, the time history of lift coefficient for both the global and truncated solutions, and contour plots comparing the full and truncated solutions.

Some comments on the results should be made. It is important to note that both the global and truncated solutions were computed independently from one another; that is, the truncated solution was not restarted from the full solution. Both solutions were started semi-impulsively from zero. The solution assumes a uniform stream as an initial condition, and the cylinder suddenly appears at time = 0. However, the code allows a slow start-up time to facilitate the calculation, whereby the velocity on the cylinder surface is gradually reduced from freestream levels to zero over the first twelve iterations. Thus, the solution is only "semi-impulsive." In addition, the code was run with a steady-state version of the algorithm to get the solution started, and then it was switched to time-accurate. It was necessary to perturb the flow in order to initiate the vortex shedding process (seen clearly in the C_L vs. time curves). Large glitches in the solution may be seen at $y = 0$, $x = 4$ in the truncated results. These are due to a programming error resulting from attempts to implicitly deal with an explicit wake cut. These errors have been fixed since the time of these plots.

The following figures were taken from slides presented at the Minisymposium on Outflow Boundary Conditions held in association with the 6th International Conference on Numerical Methods in Laminar and Turbulent Flows, Swansea, Wales, U.K., on July 10, 1989.

REFERENCES:

1. Pulliam, T. H.: Efficient Solution Methods for the Navier-Stokes Equations, The Von Karman Institute for Fluid Dynamics Lecture Series, Numerical Techniques for Viscous Flow Computation In Turbomachinery Bladings, Brussels, Belgium, January 20-24, 1986.

2. Thompson, K. W.: Time Dependent Boundary Conditions for Hyperbolic Systems, Journal of Computational Physics, Vol. 68, pp. 1-24, 1987.

VORTEX SHEDDING BEHIND CIRCULAR CYLINDER

2-D NAVIER-STOKES CODE

RE = 100

M = 0.1

$S_T = .137$

$-0.11 \leq C_L \leq 0.11$

FULL GRID EXTENDS 20 DIAMETERS

PRESSURE $C_D \simeq 1.0$

$\lambda/D = 5.3$

TRUNCATED GRID EXTENDS 4 DIAMETERS

FRICTION $C_D \simeq 0.334$

$\tau A/D = 72.75$

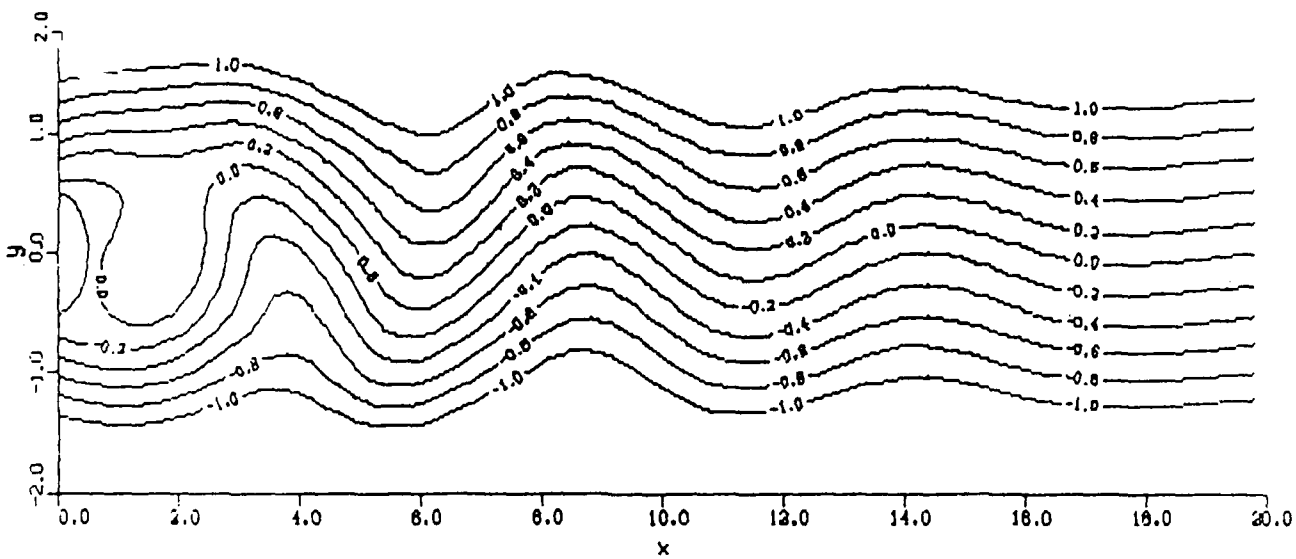

20.0
17.5
15.0
12.5
10.0
7.5
5.0
2.5
0.0
-2.5
-5.0
x
-12.5
-10.0
-7.5
-5.0
-2.5
0.0
2.5
5.0
7.5
10.0
12.5
y

5.0
4.0
3.0
2.0
1.0
0.0
-1.0
-2.0
-3.0
-4.0
-5.0
x
-5.0
-4.0
-3.0
-2.0
-1.0
0.0
1.0
2.0
3.0
4.0
5.0
y

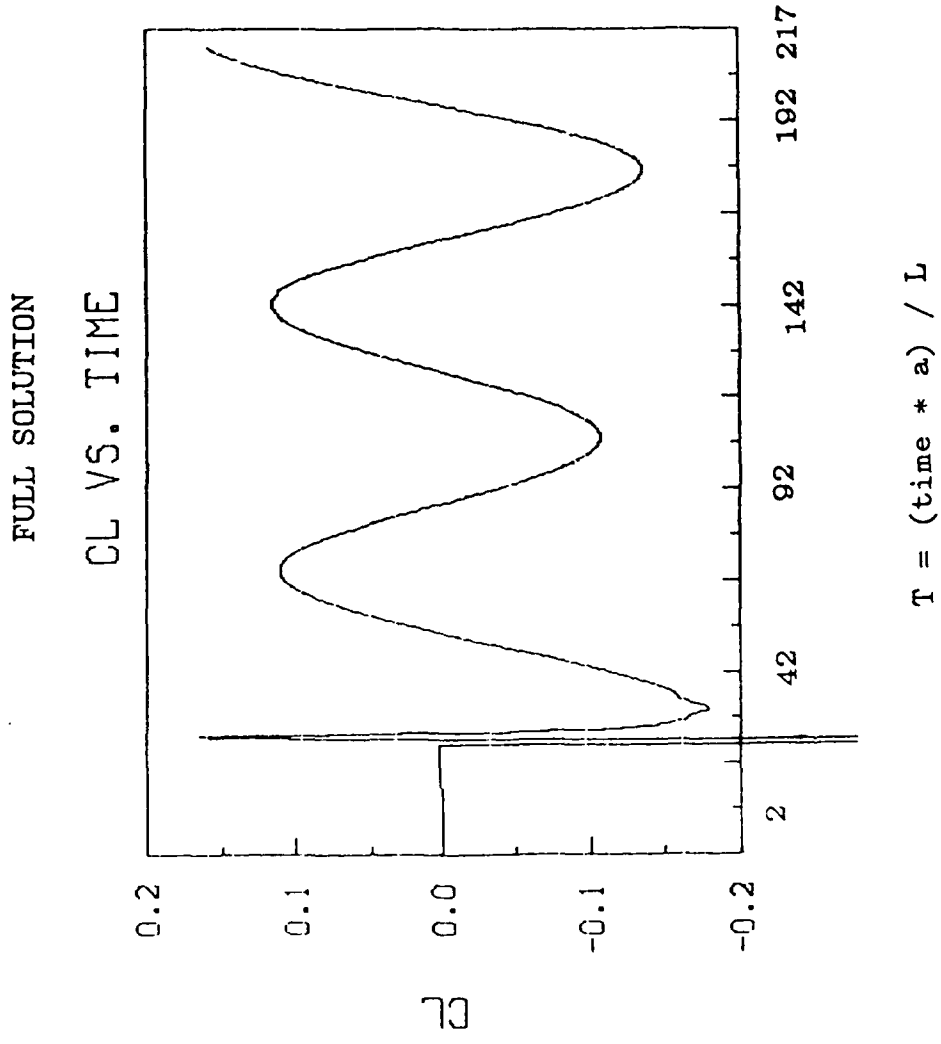
FULL SOLUTION
CL VS. TIME
CL
0.2
0.1
0.0
-0.1
-0.2
2
42
92
142
192 217
T = (time * a) / L

TRUNCATED SOLUTION

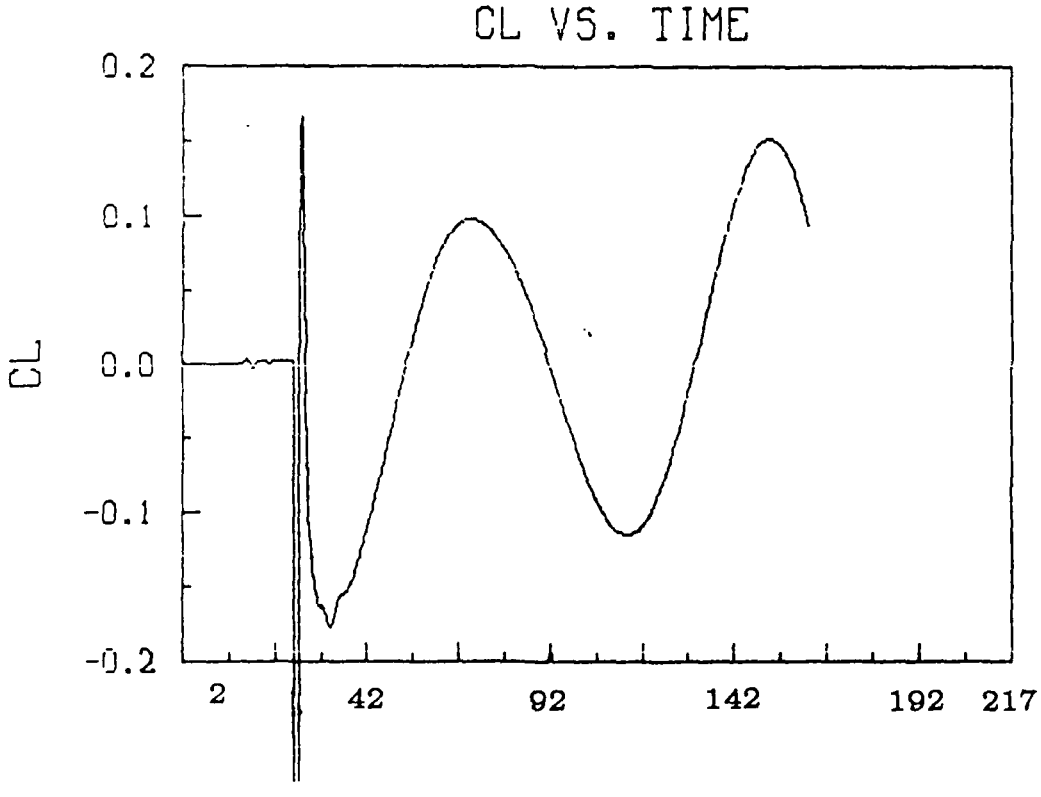

T = (time * a) / L

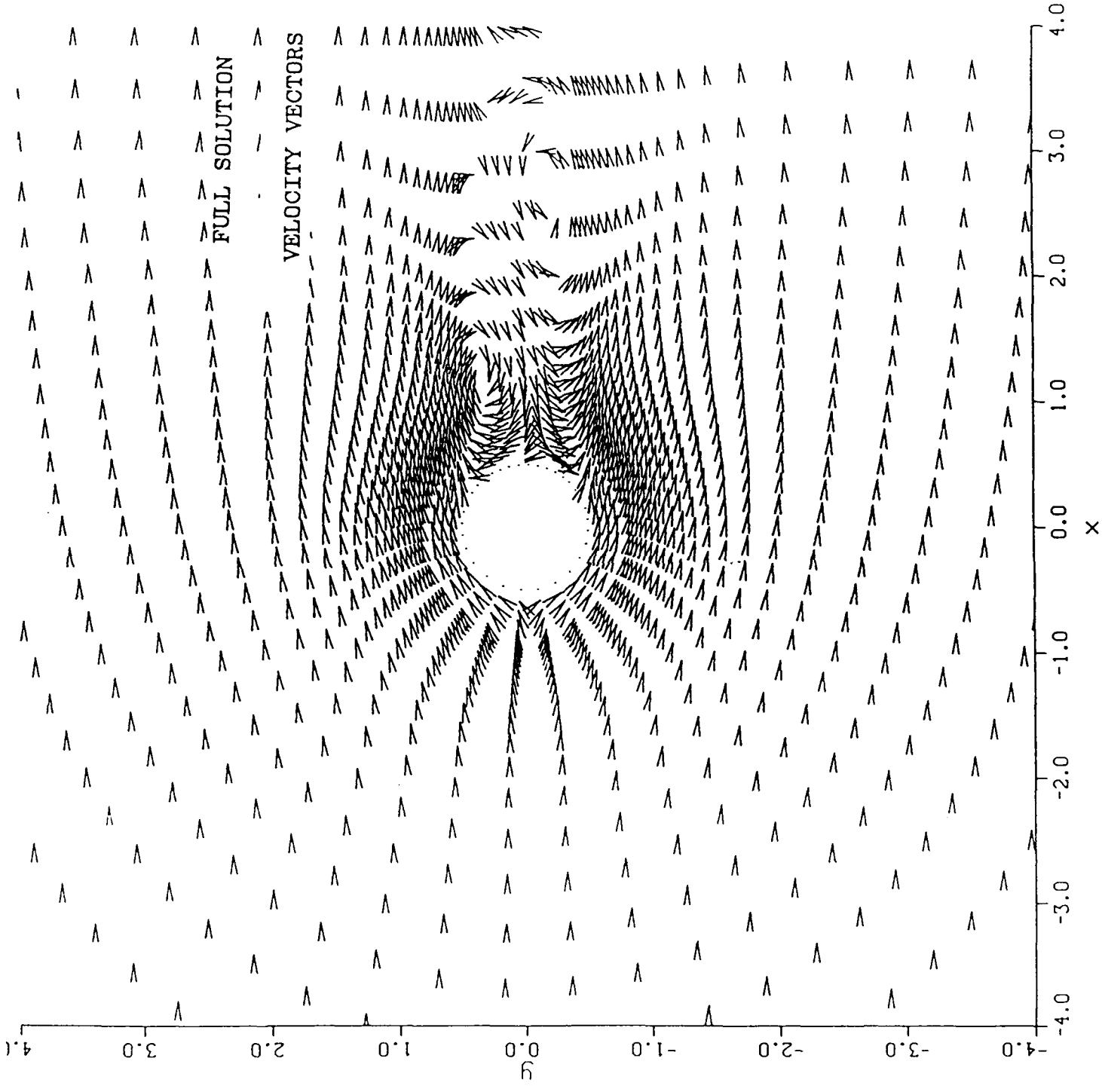
FULL SOLUTION
VELOCITY VECTORS
4.0
3.0
2.0
1.0
0.0
-1.0
-2.0
-3.0
-4.0
x
y

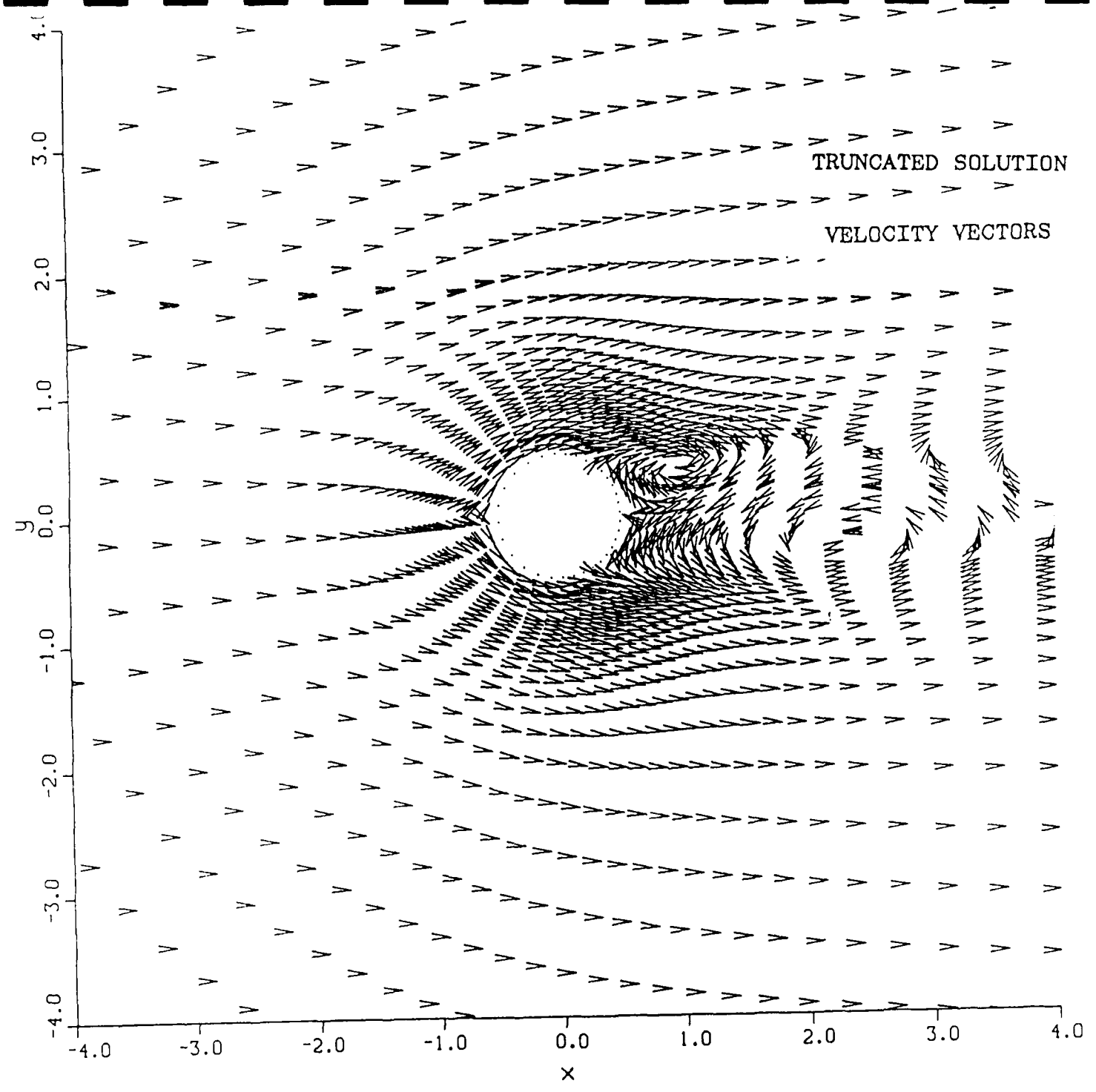
TRUNCATED SOLUTION
VELOCITY VECTORS
y
x
4.0
3.0
2.0
1.0
0.0
-1.0
-2.0
-3.0
-4.0
-4.0
-3.0
-2.0
-1.0
0.0
1.0
2.0
3.0
4.0

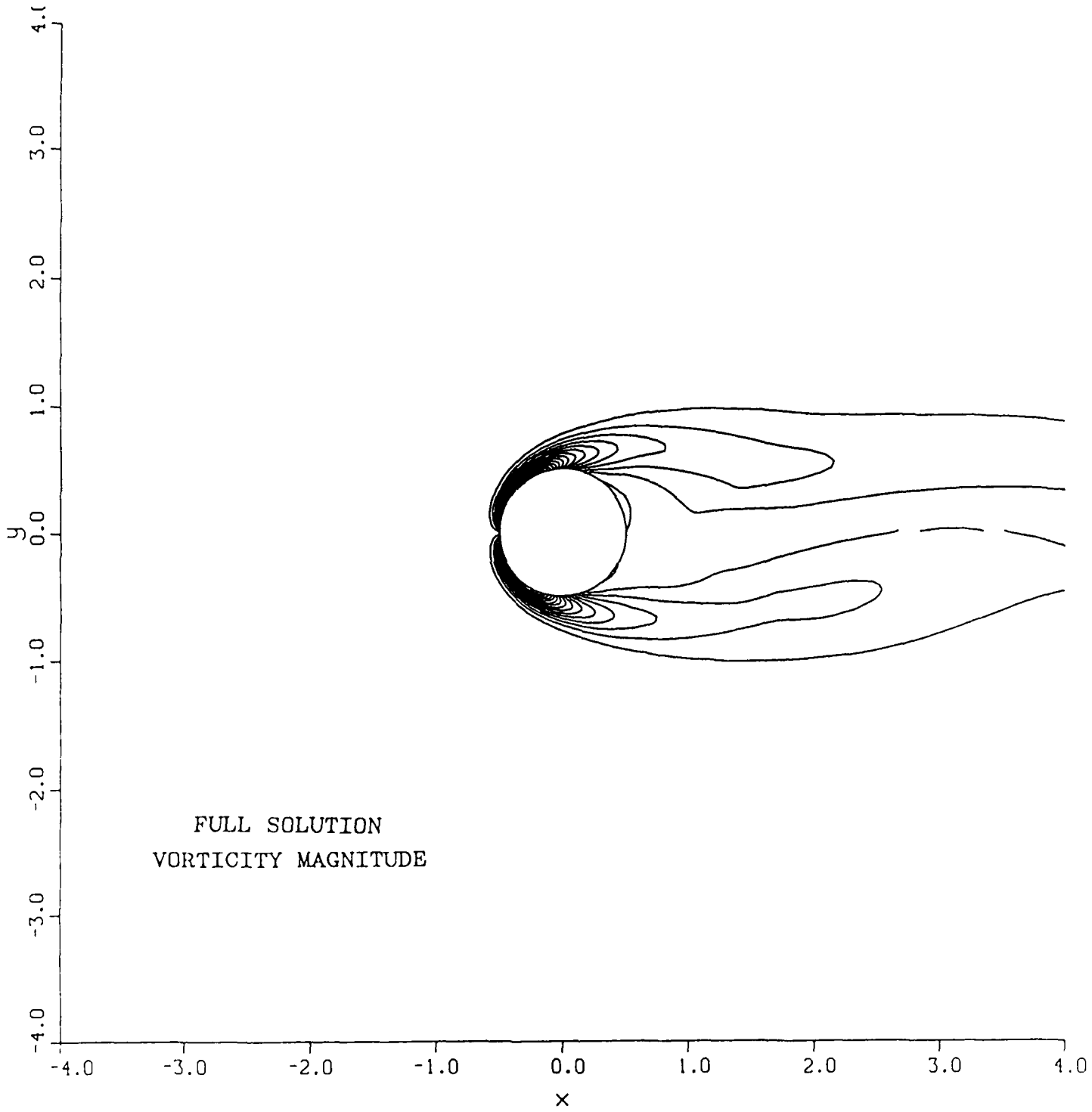
FULL SOLUTION
VORTICITY MAGNITUDE
y
x
4.0
3.0
2.0
1.0
0.0
-1.0
-2.0
-3.0
-4.0
-4.0
-3.0
-2.0
-1.0
0.0
1.0
2.0
3.0
4.0

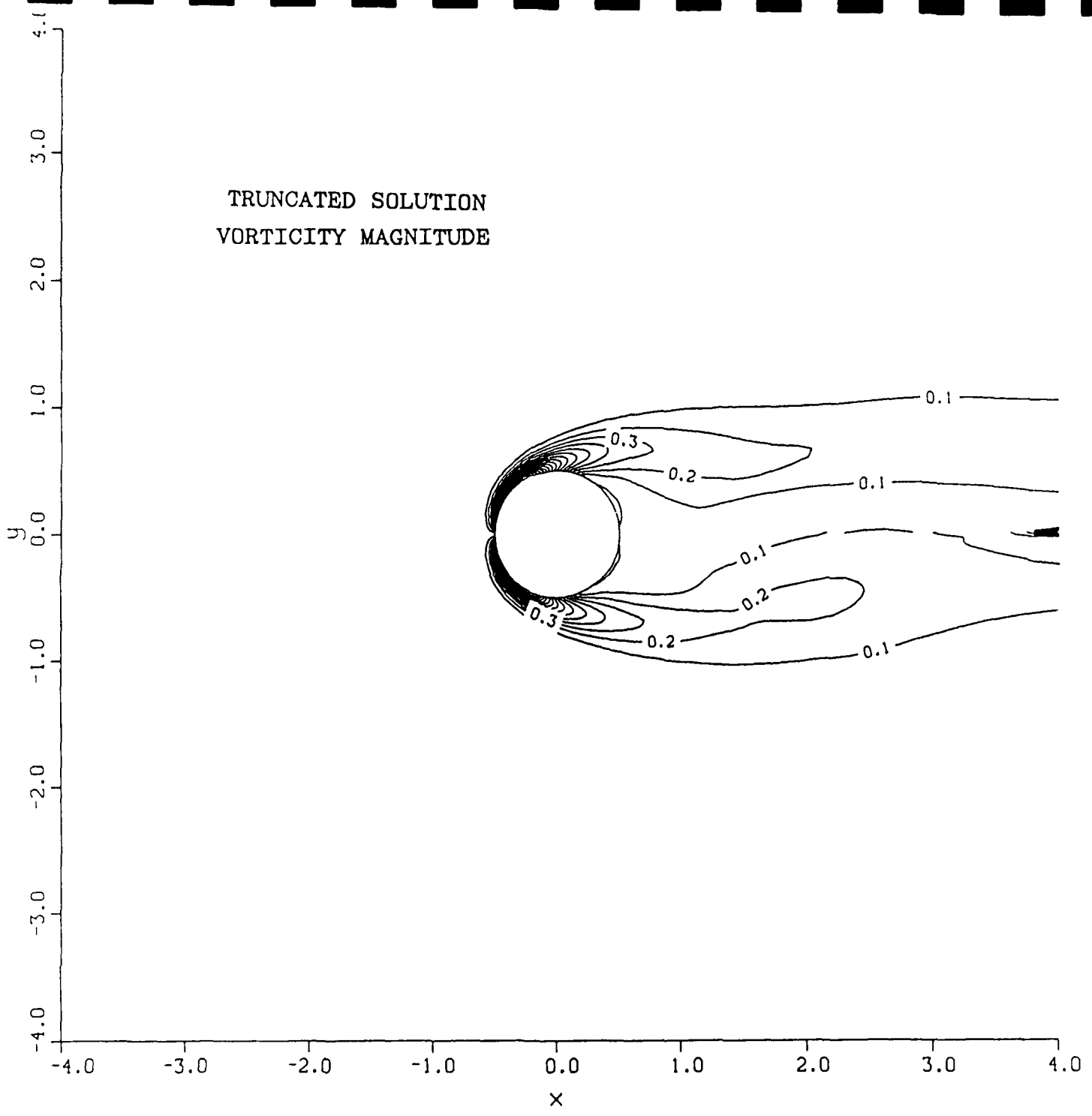
TRUNCATED SOLUTION
VORTICITY MAGNITUDE
0.1
0.3
0.2
0.1
0.1
0.2
0.3
0.2
0.1
y
x
4.0
3.0
2.0
1.0
0.0
-1.0
-2.0
-3.0
-4.0
-4.0
-3.0
-2.0
-1.0
0.0
1.0
2.0
3.0
4.0

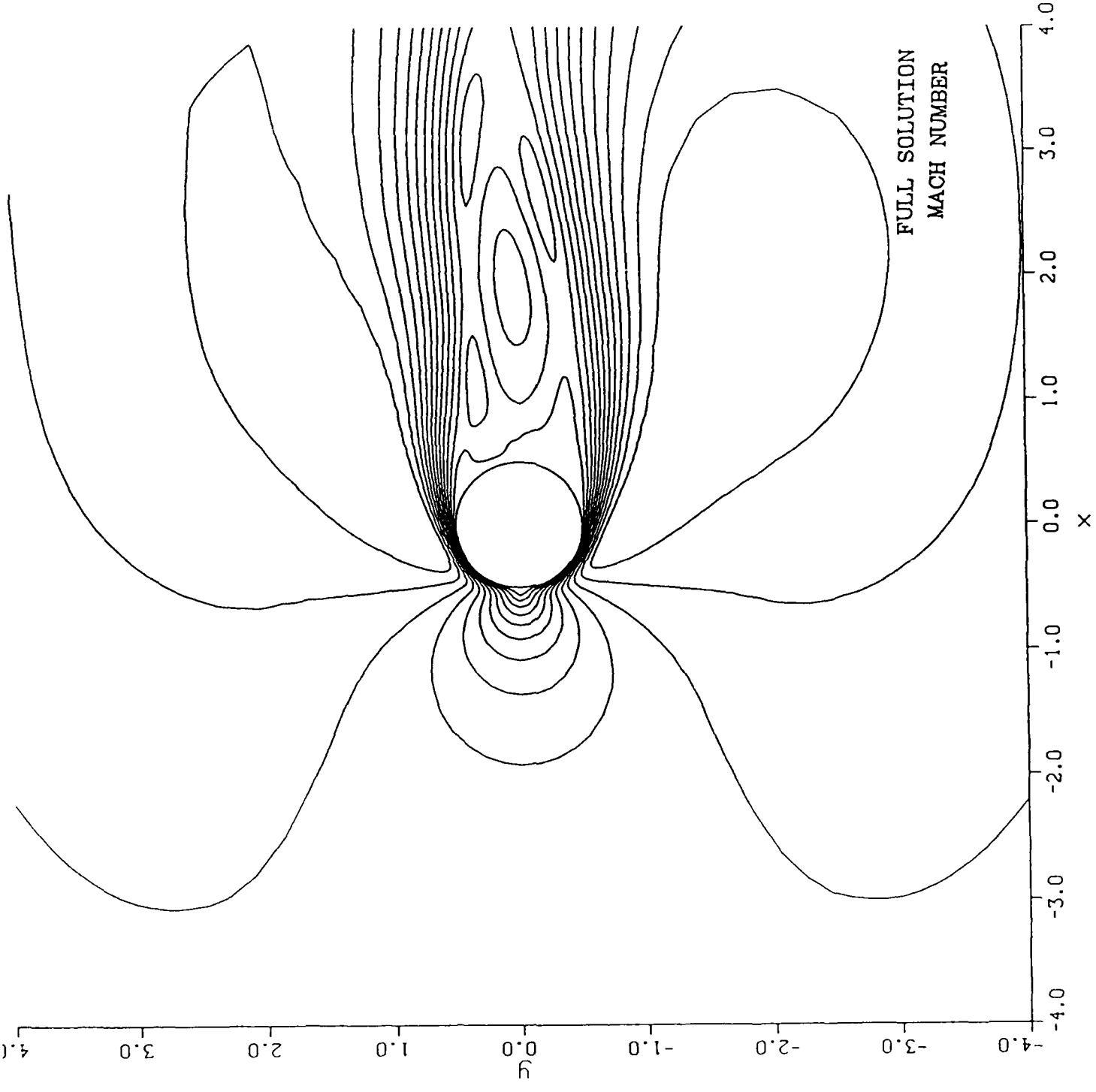
FULL SOLUTION
MACH NUMBER
4.0
3.0
2.0
1.0
0.0
-1.0
-2.0
-3.0
-4.0
x
-4.0
-3.0
-2.0
-1.0
0.0
1.0
2.0
3.0
y

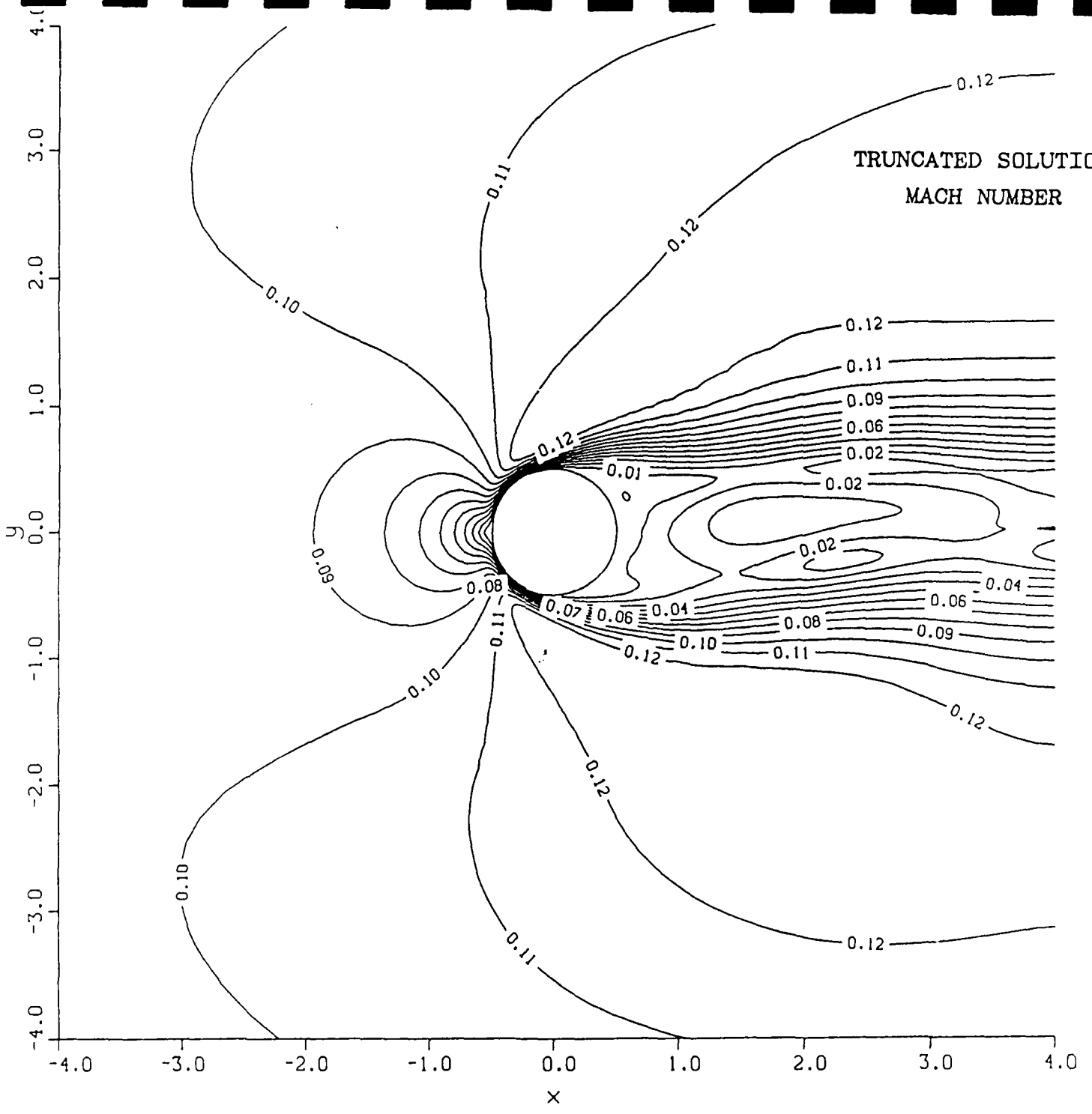
TRUNCATED SOLUTION
MACH NUMBER
y
x
4.0
3.0
2.0
1.0
0.0
-1.0
-2.0
-3.0
-4.0
-4.0
-3.0
-2.0
-1.0
0.0
1.0
2.0
3.0
4.0
0.12
0.11
0.10
0.09
0.08
0.07
0.06
0.04
0.02
0.01
0

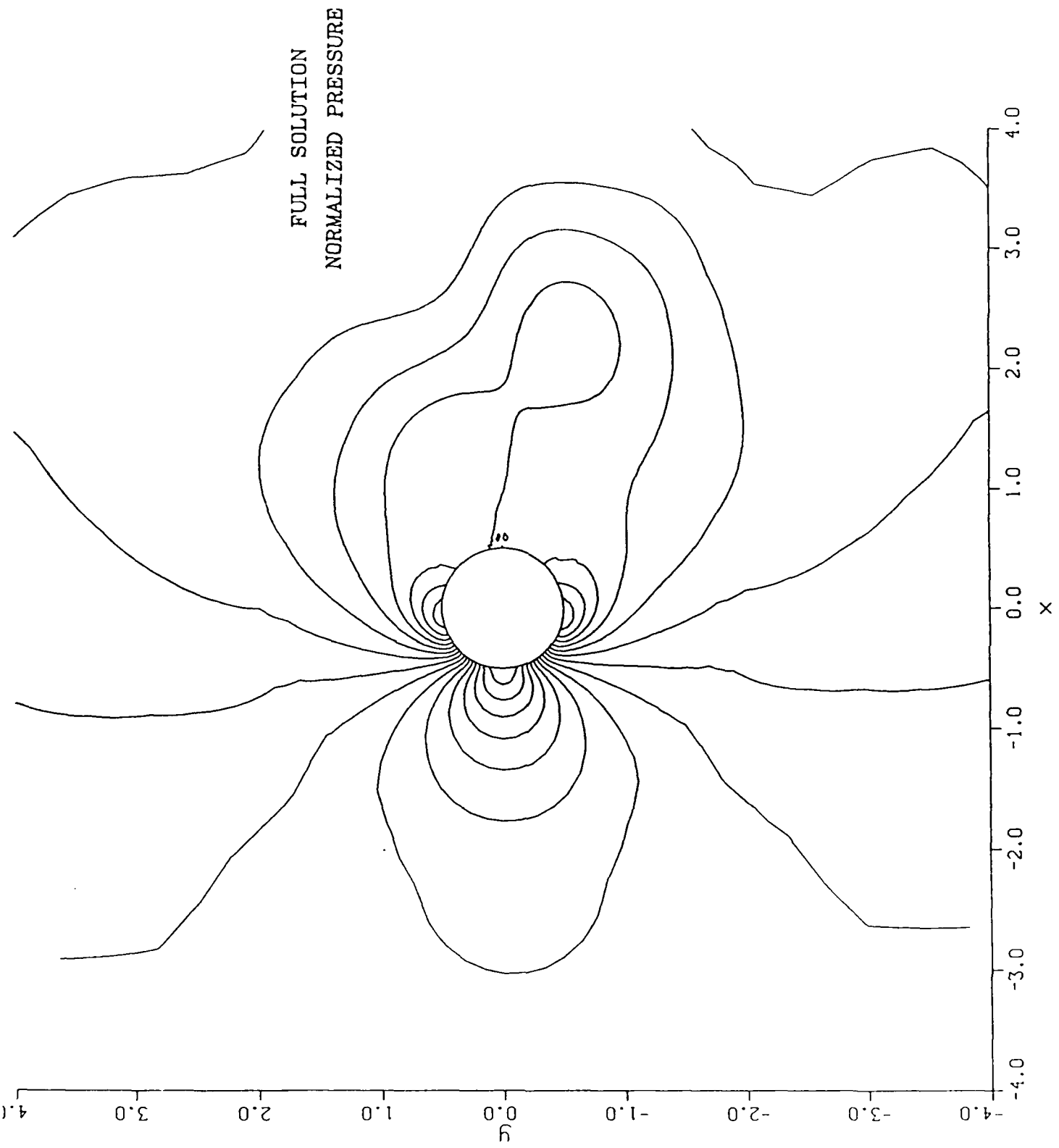
FULL SOLUTION
NORMALIZED PRESSURE
1.00
X
Y
4.0
3.0
2.0
1.0
0.0
-1.0
-2.0
-3.0
-4.0

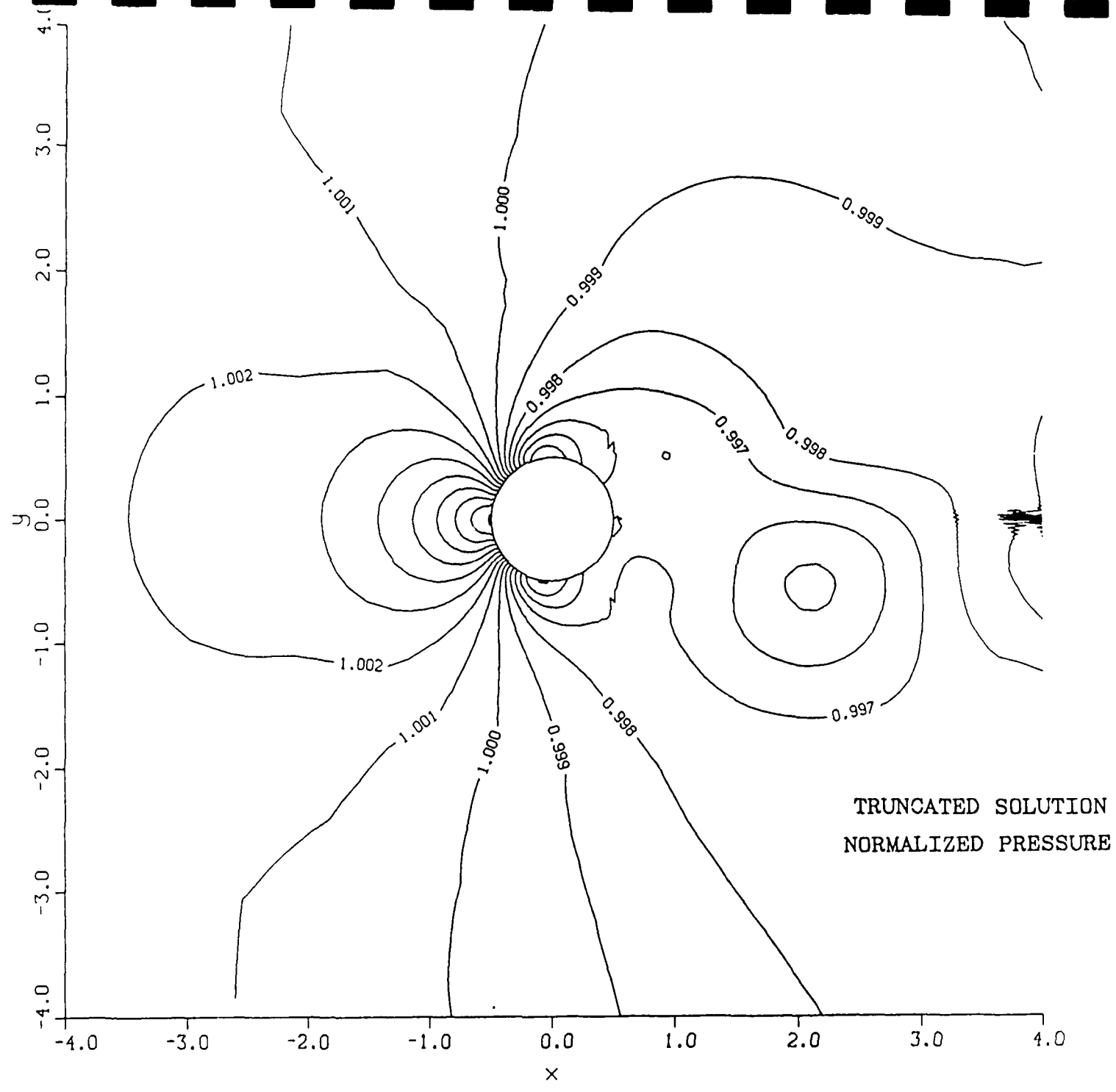
1.001
1.000
0.999
1.002
0.998
0.997
0.998
1.002
0.997
1.001
1.000
0.999
0.998
TRUNCATED SOLUTION
NORMALIZED PRESSURE
y
x
4.0
3.0
2.0
1.0
0.0
-1.0
-2.0
-3.0
-4.0
-4.0
-3.0
-2.0
-1.0
0.0
1.0
2.0
3.0
4.0

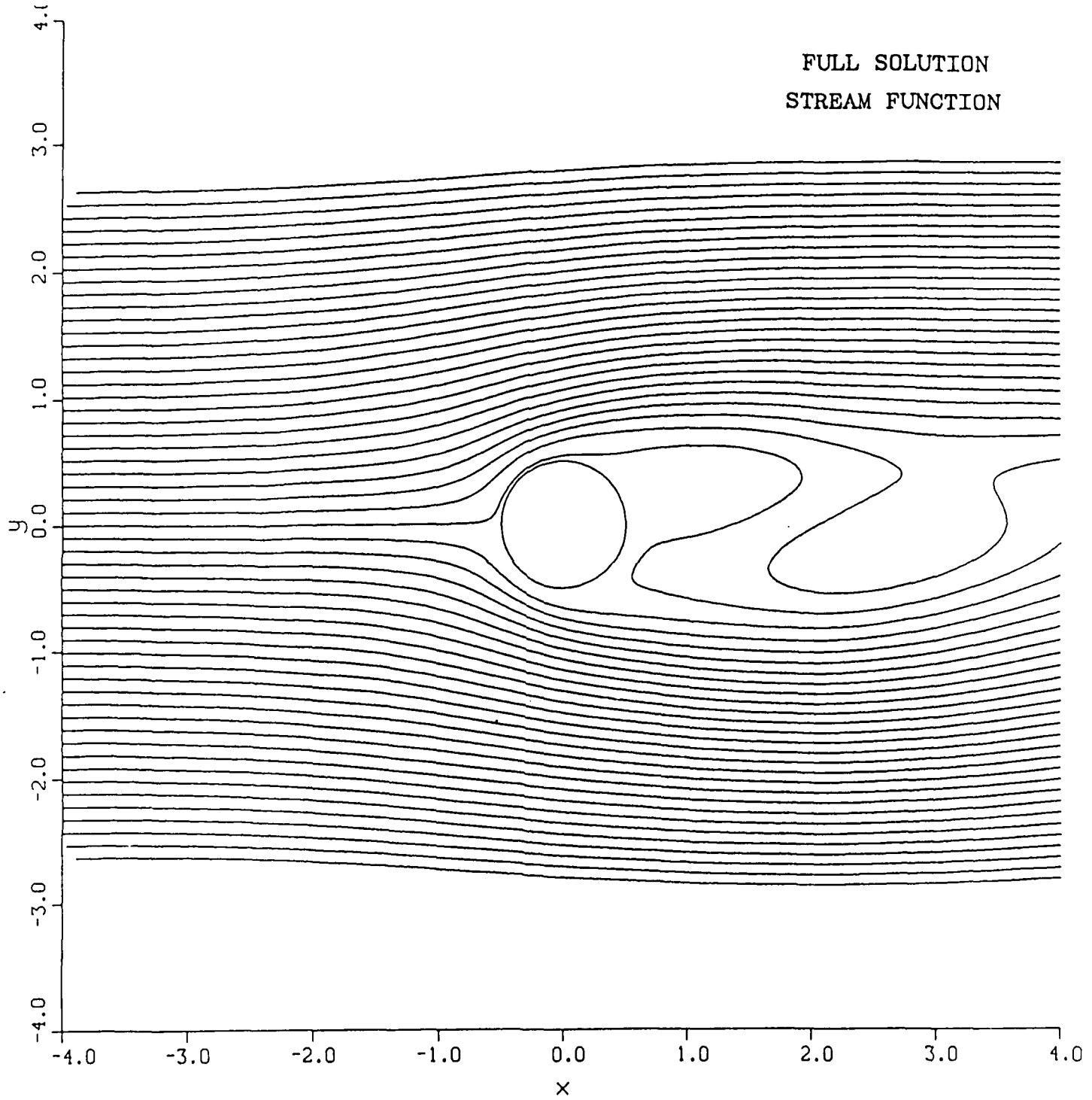
FULL SOLUTION
STREAM FUNCTION
y
x
4.0
3.0
2.0
1.0
0.0
-1.0
-2.0
-3.0
-4.0
-4.0
-3.0
-2.0
-1.0
0.0
1.0
2.0
3.0
4.0

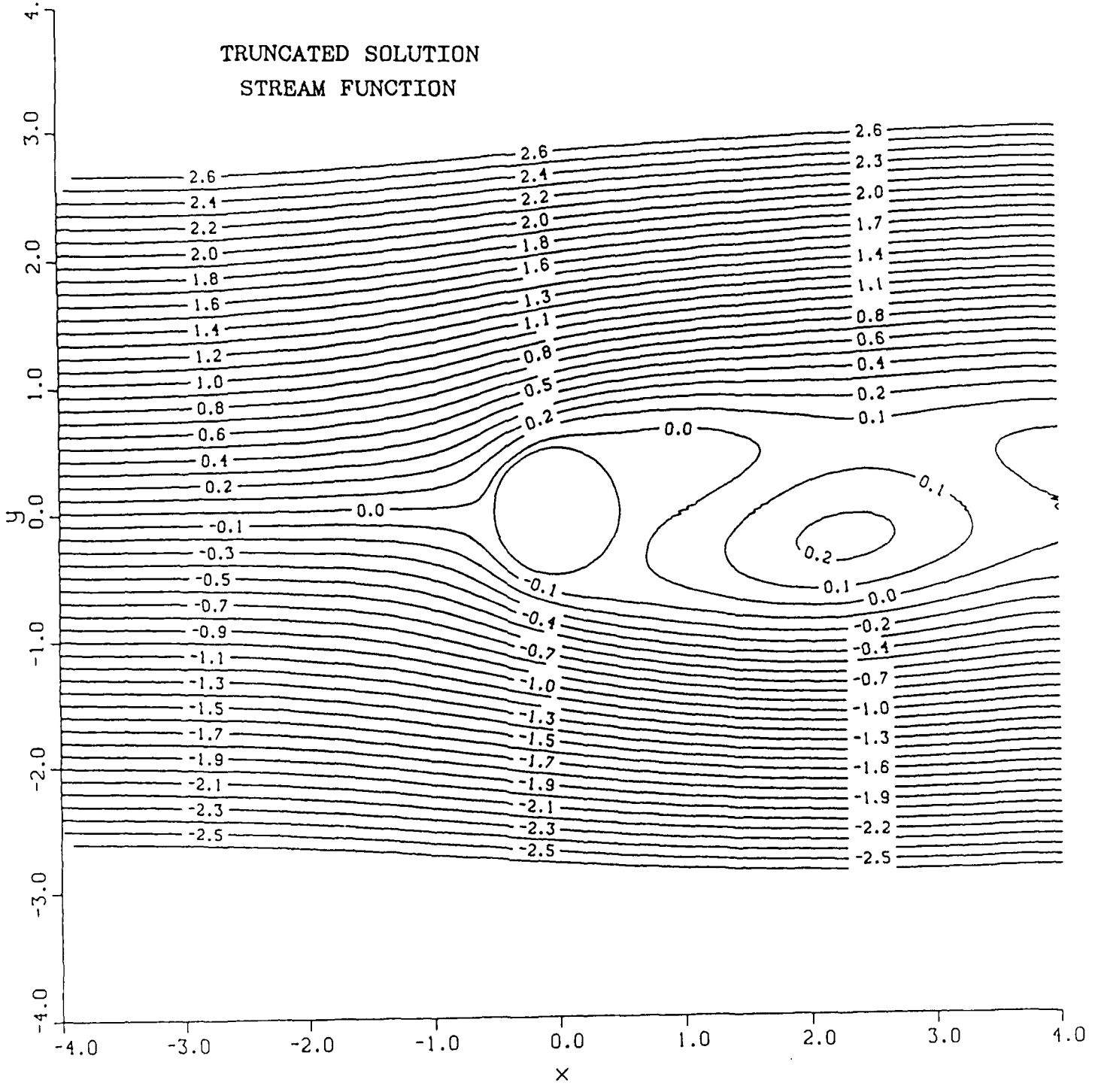
TRUNCATED SOLUTION
STREAM FUNCTION
y
x
4.0
3.0
2.0
1.0
0.0
-1.0
-2.0
-3.0
-4.0
-4.0
-3.0
-2.0
-1.0
0.0
1.0
2.0
3.0
4.0

APPENDIX D

Outflow Boundary Conditions Using Duhamel's Equation

INTRODUCTION

A problem that has existed in computational fluid dynamics (CFD) since its inception is in selecting the correct boundary conditions for an outflow boundary. An outflow boundary is one through which the flow exits the computational domain. The errors introduced by an inadequate boundary condition can range from a progressively inaccurate but physically realistic solution to a nonphysical solution. The nonphysical solution can arise because the boundary condition represents the effect of the unknown on flow outside the computational domain, and if the "exterior" flow is nonphysical, then the "interior" flow is nonphysical. A simple example of such a situation occurs when a steady state asymptotic boundary condition is used for an unsteady problem. In this case all unsteadiness in the interior flow will vanish before the boundary or the frequency of the unsteadiness will adjust such that the boundary is a node in wave space; either of these situations is nonphysical. In general, the errors introduced by the outflow boundary condition are greatest for unsteady flows.

The early attempts at finding suitable outflow boundary conditions concentrated on using asymptotic solutions of simpler flow models, which could be obtained analytically. For example, analytic solutions of the Prandtl-Glauert equation were used as boundary conditions for the transonic small disturbance equation. However, the usefulness of this idea is limited because of the difficulty in finding analytic solutions that will model the outflow for the Navier-Stokes or Euler equations.

An alternative to asymptotic solutions is the idea of nonreflecting boundary conditions. The physical basis of the idea is that outgoing waves cannot be reflected at an (artificial) computational boundary. A one-dimensional analysis was developed by Enquist and Majda[1] for the unsteady Euler equations, and a version for the unsteady transonic small disturbance equation was developed by Kwak.[2] The ideas have been extended to two dimensions by Thompson,[3] but the theory is really a composite of two one-dimensional solutions. Rodman[4] has extended this idea to curvilinear coordinates, but again the two-dimensionality is "decoupled."

If a particular flow is started from zero, then the flow in the exterior domain is exact until waves from the disturbance in the interior domain cross the boundary. If true nonreflecting boundary conditions could be devised, then the outflow boundary condition would be correct if the computation was started at zero time and is time accurate. An error in the boundary conditions due to approximations in the formulation can give rise to a nonphysical flow in the exterior domain and hence, ultimately, the interior domain. A principal difficulty is in finding an analytic relationship that will give the boundary conditions for the Navier-Stokes equations. The progress in nonreflecting boundary conditions shows that finding a true two-dimensional boundary condition is beyond the present state of the art.

The domain to the right of AB is the exterior domain, that to the left of CD, the interior domain. There is an overlap of width one grid cell in the x direction.

The object is to find the boundary condition on CD based on information on AB. Note that the flow in the exterior domain is defined solely by the correct data on AB.

If the flow in the exterior domain can be represented by a time linearized equation with a boundary condition, $U_j(t)$ on AB, where U_j is constant over the jth grid cell in the y direction, then the value of $U_k(t)$ on CD at the kth grid cell is given by Duhamel's equation

$$\tilde{U}_k(t) = \sum_{j=1}^{N} \left\{ U^{(\varepsilon)}_{jk}(t)\,\varepsilon_j(o) + \int_o^t U^{(\varepsilon)}_{jk}(t-\tau)\,\frac{d\varepsilon_j(\tau)}{d\tau}\,d\tau \right\} \qquad (1)$$

where $U^{(\varepsilon)}_{jk}(t)$ is the "indicial response" of U on CD at y_k, that is, the transient due to a unit step change in the boundary conditions on AB at y_j, $U_j(t)$. $\varepsilon_j(t)$ is the actual value of $U_j(t)$ from the interior section. The indicial response is obtained by running the CFD code to be used in the analysis over a large domain with a step change in U_n at time zero and some y station y_j, and

$$U_i(t) = 0 \quad i \neq j \qquad (2)$$

where $U_i(t)$ denotes a value at y_i. The time transient on the grid points on CD, y_k, are stored and, when divided by the magnitude of the step, becomes the indicial response $U^{(\varepsilon)}_{jk}(t)$. In principle, this should be computed for all the j stations on AB and constitutes a formidable mass of information. However, certain simplifications can be made. First, since there is no origin on the infinite boundary, AB, all that matters is the location of the y_k point relative to the location of the step change, that is, the difference $y_k - y_j$, and hence the indicial response for the jth point on AB is the same as for any other cell provided the difference $y_k - y_j$ and the cell width is held constant. The cell used to impose the step change may be thought of as the base cell. This removes the amount of stored data by a factor of N, the number of y grid points. If a variable grid is used then the effects of varying grid size on $U^{(\varepsilon)}_{jk}$ can be constructed by a sum of the indicial responses of the base cell. Secondly, the time variation can be approximated by curve fits which work quite well. [5] This removes the necessity to store every time step; only the coefficients of the approximating series need be stored. In the examples shown here this second simplification

In Figure 1 the lift coefficient variation for the first cycle for the transonic case, $M_\infty = 0.8$, is shown; the boundary is 0.25 chords downstream of the airfoil. The standard code for the truncated grid diverges at 150 time steps. The reason is indicated in Figure 2 where the pressure distributions are shown. It can be seen that the nonreflecting boundary conditions are totally inadequate.

CONCLUDING REMARKS

A new treatment of outflow boundary conditions is outlined and some preliminary results are shown. The technique is applicable to a wide range of equations, including the Navier-Stokes equations.

REFERENCES

1. Enquist, B. and Majda, A.: Numerical Radiation Boundary Conditions for Unsteady Transonic Flow. J. Comp. Phys., Vol. 40, No. 1, 1981.

2. Kwak , D.: Nonreflecting Boundary Conditions for Unsteady Transonic Flow Computations. AIAA Journal, Vol. 19, No. 11, 1981.

3. Thompson, K. W.: Time Dependent Boundary Conditions for Hyperbolic Systems. J. of Comp. Phys., Vol. 68, 1987.

4. Rodman, L. C.: The Application of Non Reflecting Boundary Conditions to 2-D Unsteady Computations on Curvilinear Grids. (Submitted to AIAA 21st Fluid & Plasma Dynamics Conference).

5. Nixon, D. and Tzuoo, K-L.: Prediction of Gust Loading and Alleviation at Transonic Speeds. J. Aircraft, Vol. 24, No. 10, 1987.

6. Whitlow, W.: XTRAN2L - A Program for Solving the General Frequency Unsteady Transonic Small Disturbance Equation. NASA TM 85223, 1983.

APPENDIX E

A Characterization and Search Technique for Unsteady Flow Control Problems

One objective of the proposed work was to use an optimizer to determine the best boundary conditions for controlling a flow field. Mathematical optimizers were available for this purpose, but they have several disadvantages which made them ill-suited to this problem. Consequently, an alternative method was developed which could characterize the solution that was being optimized, so that information about all aspects of the solution would be found. For instance, various solution trends could be documented as they were discovered, providing information that would help in the search for a new optimum if the problem criteria were changed.

Mathematical optimizers, such as CONMIN,[1] require the definition of an objective function which is to be minimized by the code. Then, the inputs upon which the objective function depends are varied, starting from an initial position, and an optimum combination of the inputs is found. One usual drawback to these optimizer codes is that only the closest local minimum of the objective function will be found, therefore requiring several restarts of the code with different initial inputs if the problem is suspected to have more than one local minimum. Another disadvantage is that all quantities of interest must be represented by one function to be optimized, resulting in the loss of information about how they are affected individually by the inputs. A third drawback to these optimizers is that the answer alone is given, without significant other information, such as how each individual input affected the answer, and if there were any regions of unusual or rapid change in the solution field.

The current technique was developed to address some of these disadvantages. It is used as a postprocessor to CFD results. A number of inputs to the problem may be used, and rather than one objective function, several quantities of interest may be specified independently. A representative sample of inputs is used with the CFD code, and the corresponding quantities of interest are generated as outputs. The postprocessor for this information has programmed into it the heuristic rules that a person would follow if solving the same problem. The change in the flow solution as a function of one of the variables, with the other variables remaining fixed, is found for all combinations of the variables. The effect of one variable on the solution may be found to be independent, mildly dependent, or strongly dependent upon the other variables. In addition, how fast the solution changes with a given variable is found. These computed slopes indicate whether a dependence is linear and/or monotonic. The relationships between the flow solution and the input variables, along with any regions of high nonlinearity or non-monotonicity, are documented by the code. These results give insight into the cause-and-effect relationships between the various flow variables and computed flow field.

The postprocessor may be run iteratively with the CFD solver to find an optimum for each flow quantity, or it may be used as a characterization code alone if an optimization is not required. For optimization, two techniques are used to guide the search. First, a basic hill-climbing technique is used, where the region surrounding the current optimum is investigated for incremental improvements. Additionally, any exceptional areas, as

shown in the plots to indicate where this happens. In Figure 2, a double bar is shown between the first and fifth plot, where the function changes from "other" to "convex."

The code then determines where future data points should be taken, both to search for an optimum and to investigate potentially interesting regions with more detail. The suggested values for future iterations are based on three criteria. First, the program looks in the vicinity of the current optimum. It uses information about the slopes and the clrms value in that area to indicate how big a jump the next iteration should take. The code checks to see if the slope in that area is much higher than the median slope throughout the solution field. It also checks to see if the optimum value found is much higher than the median value throughout the solution field. If the local slope or clrms value is not significantly larger than the median slope or clrms value, then a relatively large increment will be chosen for the next iteration. If the local slope and clrms value are high, then a smaller increment will be chosen, especially if the code determines that the next iteration will fall in uncharted territory. If the next iteration would be in an area previously investigated, no new move is indicated.

The second criteria for future iteration is based on unusual slopes in the solution field. If a particular slope is much higher than the adjacent slopes, or is much higher than the median slope, a new point is suggested that is in the direction of most improvement. The third criteria is based on mismatched functions between adjacent regions. If they exist, points between the two regions are suggested for future iteration. In Figures 2-4, suggestions for future iterations are plotted on the horizontal axes. A square indicates a search about the local optimum, a circle indicates a search based on unusual slopes, and a cross indicates a search based on mismatched functions.

Two iterations were performed after the initial twenty runs, and the results are shown in Figures 5-7. With this much data, it can be seen that there are regions where clrms is very sensitive to the input variables and that more resolution is necessary to understand the results. The code is programmed to flag any regions where it is necessary to increase the resolution. If a strong dependence on either q2 or q3 within one region shown in Figure 5 is found, then that region should be subdivided, so that each resulting subdivision is independent of q2 and q3. In this example, the code found that the region where q1 is high, q2 is low, and q3 is low needs more resolution. That one region is then subdivided, and the results are shown in Figures 8-10.

The most favorable combination of inputs for reducing the rms lift coefficient was a low suction magnitude with short duration and interval pulses. Figure 11 shows the lift coefficient history for this case. Compared with the no-slip boundary condition case shown in Figure 1, the rms lift coefficient was decreased by 10%, from 0.178 to 0.159, and the average lift coefficient was increased by 5%, from 0.977 to 1.022.

This method also investigated the region where the solution was most sensitive to the inputs, even though that region did not correspond to the optimum values found. The characterization showed that the rms lift coefficient is most sensitive to long blowing durations, short intervals between blowing pulses, and high suction values. In that region, the most interesting result was found where the combinations of inputs gave a maximum rms lift coefficient. The lift coefficient history is shown in Figure 12. Although the objective

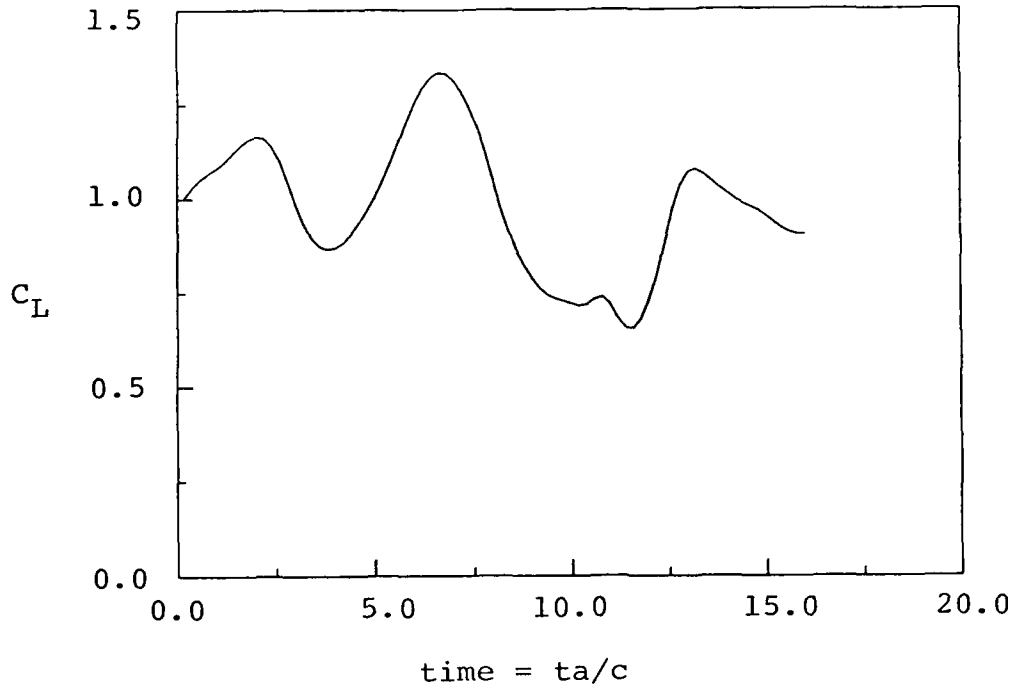

Figure 1.- Lift coefficient history for no-slip boundary conditions.

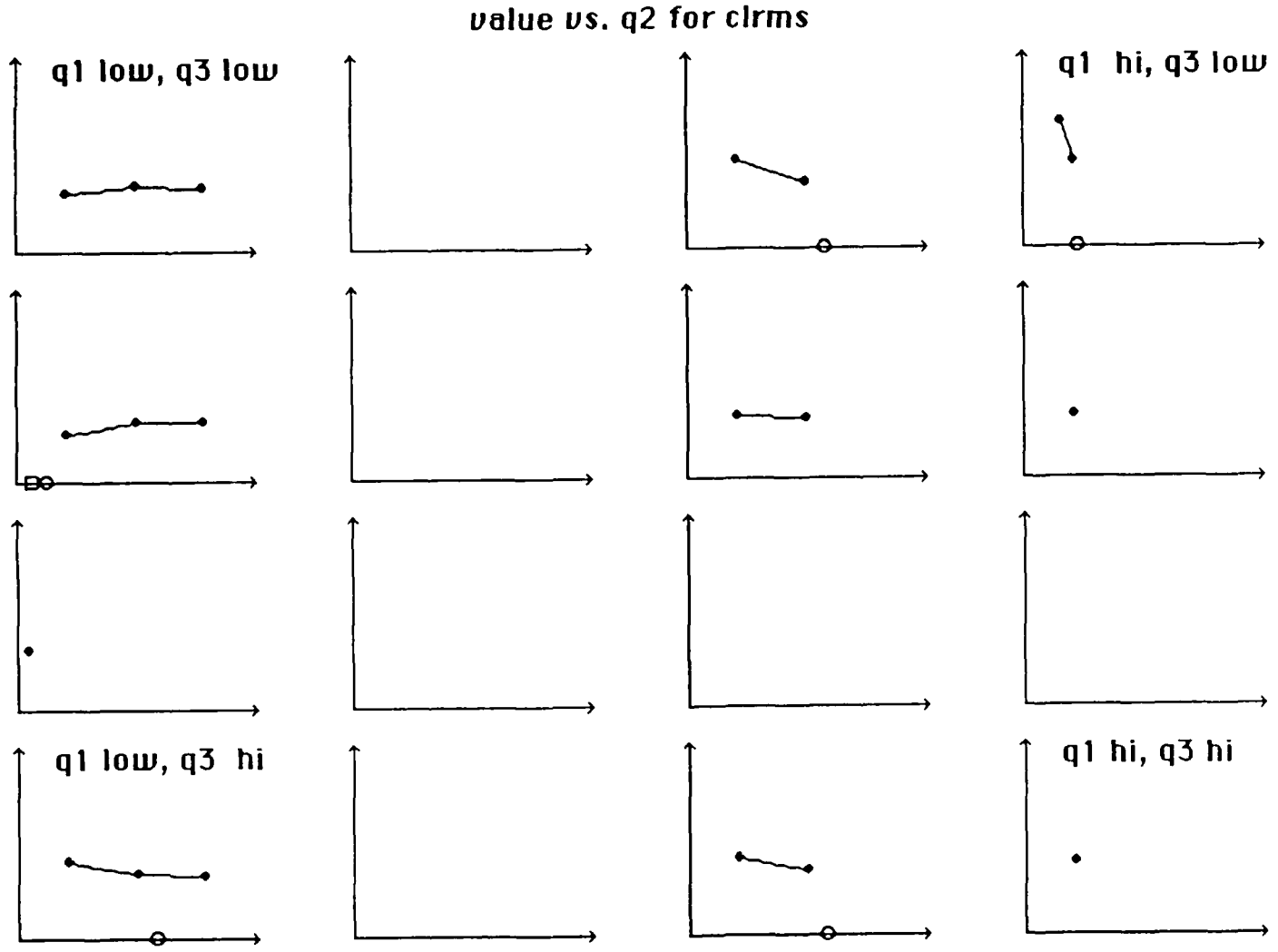

Figure 3.- RMS lift coefficient value vs. pulse interval (q2). Blowing duration (q1) and magnitude (q3) are approximately constant for each plot. Full domain, first iteration.

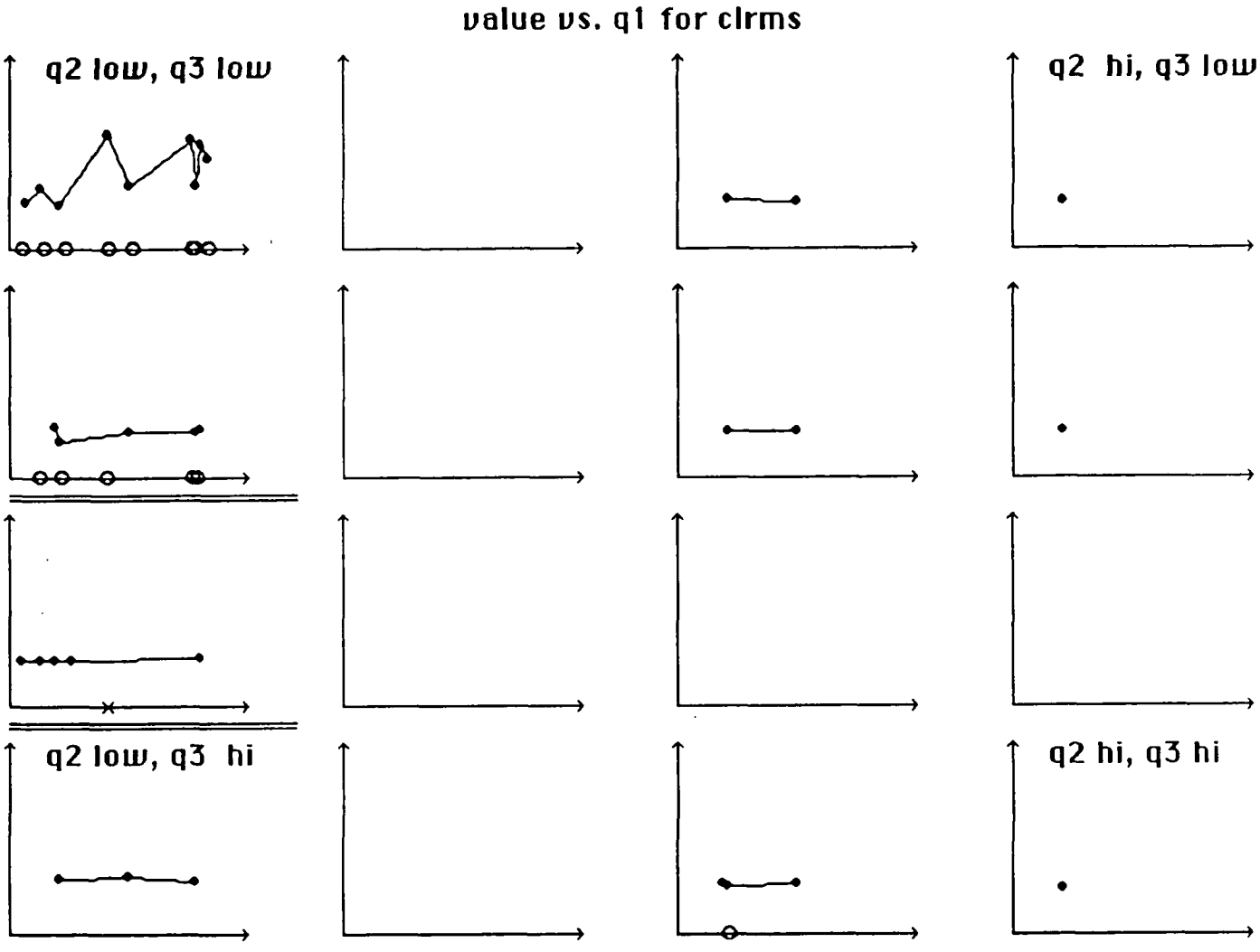

Figure 5.- RMS lift coefficient value vs. blowing duration (q1). Pulse interval (q2) and magnitude (q3) are approximately constant for each plot. Full domain, third iteration.

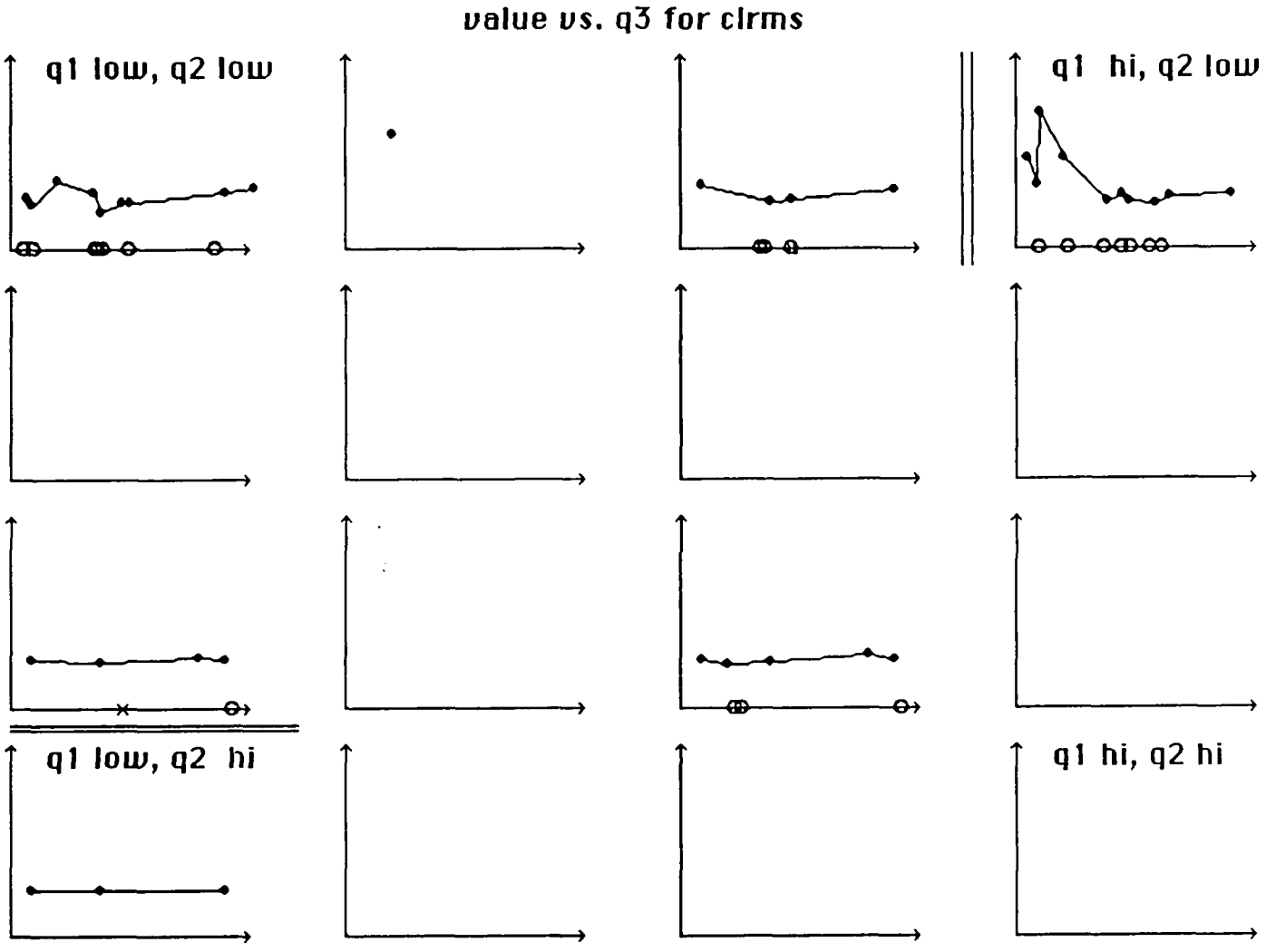

Figure 7.- RMS lift coefficient value vs. blowing magnitude (q3). Blowing duration (q1) and pulse interval (q2) are approximately constant for each plot. Full domain, third iteration.

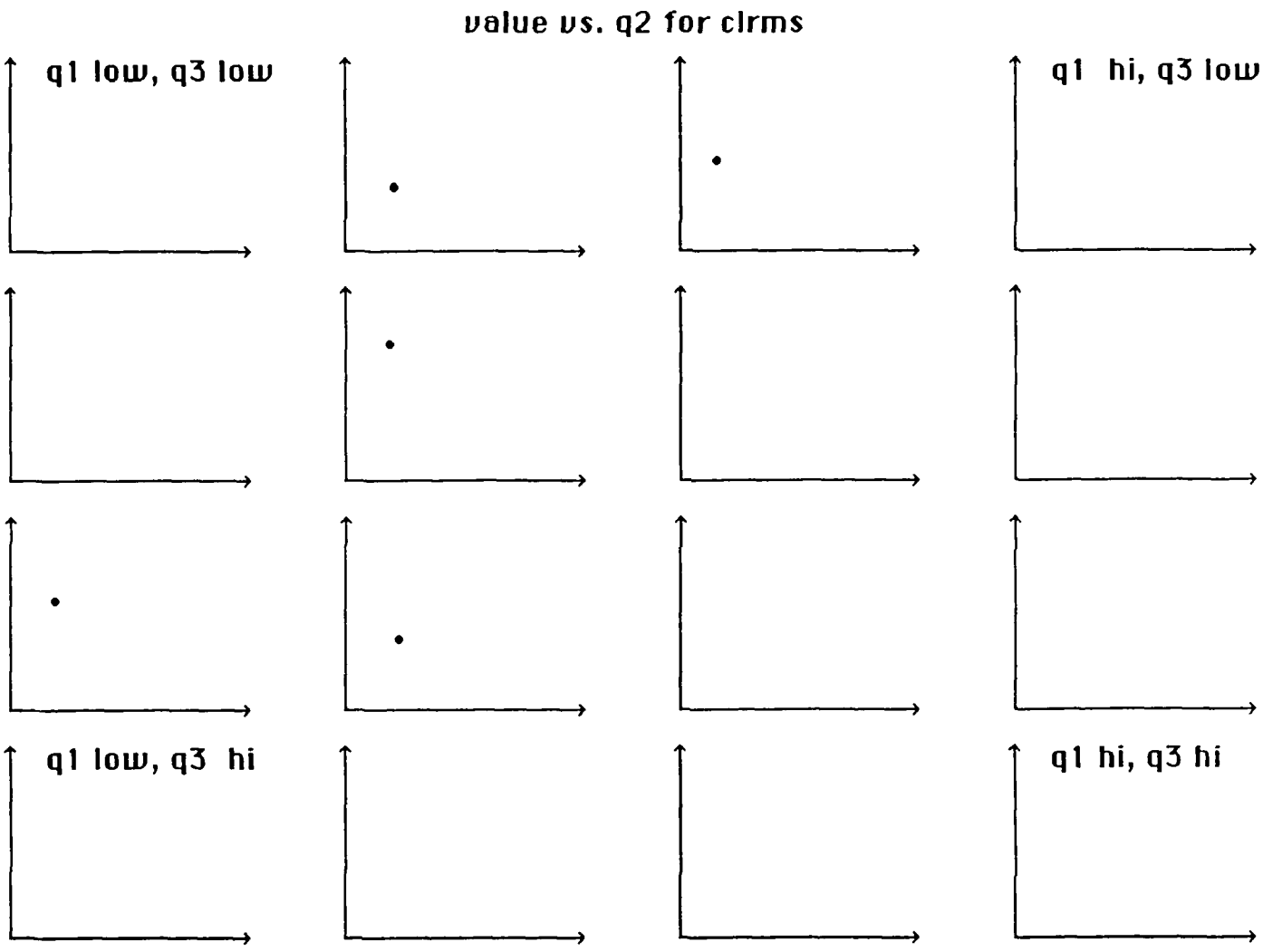

Figure 9.- RMS lift coefficient value vs. pulse interval (q2). Blowing duration (q1) and magnitude (q3) are approximately constant for each plot. Partial domain, third iteration.

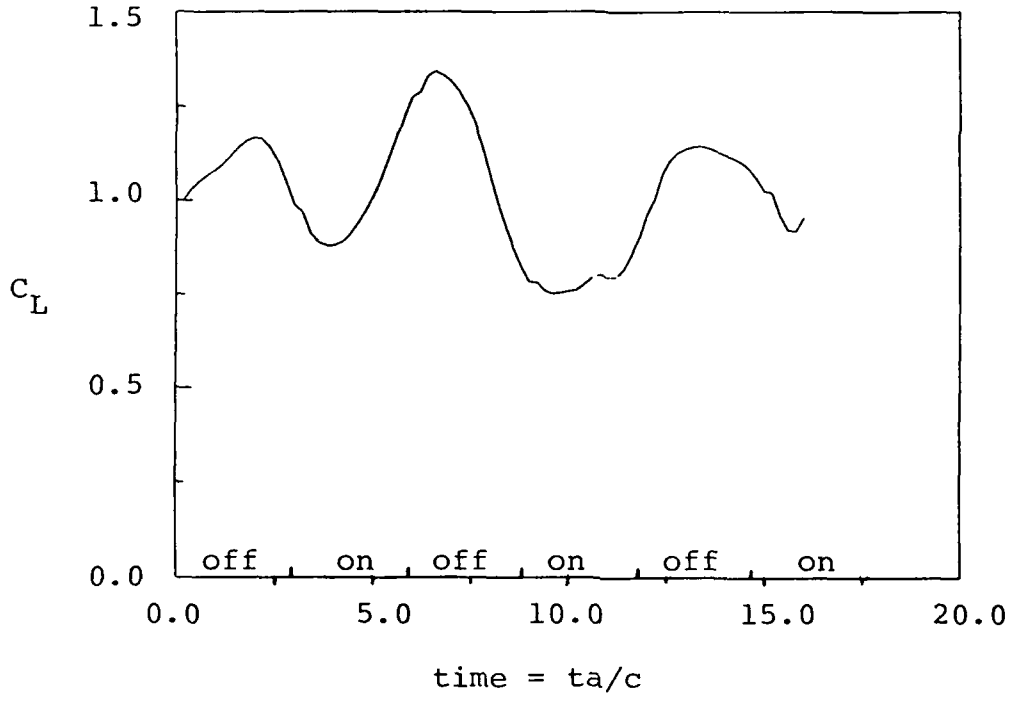

Figure 11.- Lift coefficient history for pulsed suction boundary conditions. *Suction* = $-0.05*M_\infty$.

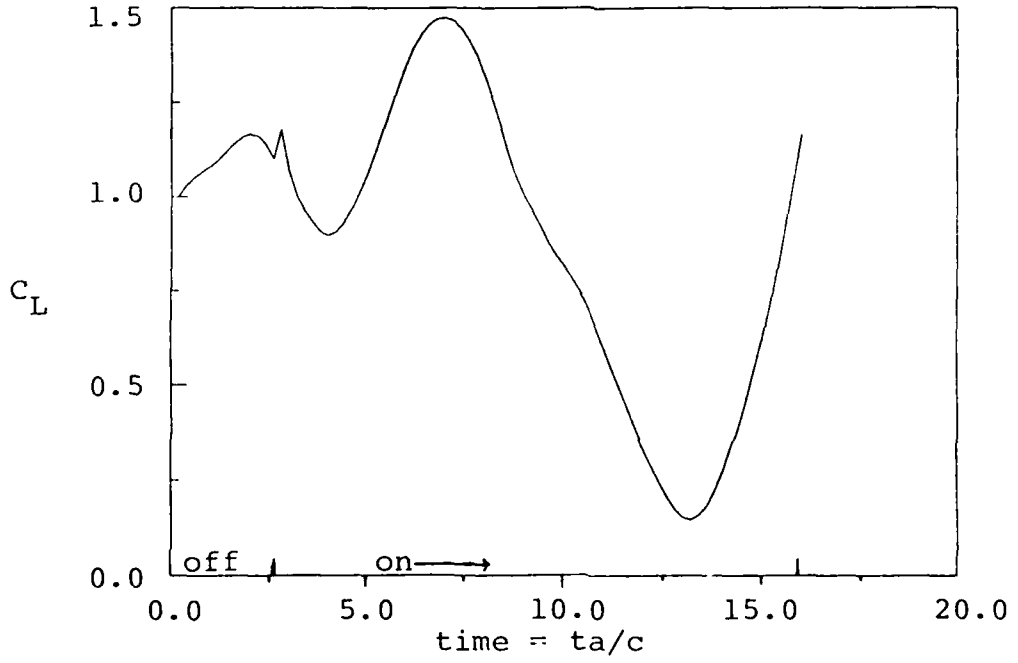

Figure 12.- Lift coefficient history for pulsed suction boundary conditions. Suction = $-0.174*M_\infty$.